A

THESIS

SUBMITTED IN PARTIAL FULFILMENT OF THE REQUIREMENTS

FOR THE HONORS DEGREE OF

BACHELOR OF SCIENCE IN PHYSICS

High Energy Neutron Detection for LENS

Jonathan Horton

DEPARTMENT OF PHYSICS
INDIANA UNIVERSITY

May 23, 2005

Supervisor: _____

Signature
Typed Name: Prof. Hermann Nann

Co-signer: _____

Signature
Typed Name: Prof. Hans-Otto Meyer

High Energy Neutron Detection for LENS

Jonathan Horton

Prof. Hermann Nann
Prof. Hans-Otto Meyer

May 23, 2005

Abstract

Results of an undergraduate research project to detect neutrons generated by the Low Energy Neutron Source at the Indiana University Cyclotron Facility are reported. Basic fast electronic schemes for neutron detection are set up and tested. Several methods of spectral analysis for scintillators are investigated. Possible arrangements of plastic scintillators are modelled using Monte Carlo techniques. This Monte Carlo program should justify spectrum unfolding via the reverse process of folding a spectrum.

1 Introduction

The Low Energy Neutron Source (LENS) has recently been commissioned at the Indiana University Cyclotron Facility (IUCF). A 7 MeV proton beam is generated and hits a beryllium target, which gives off neutrons. These neutrons proceed through a moderator and down designated beam pipes. With the neutrons are gammas from the ^{9}Be(p, $\alpha\gamma$)^{6}Li reaction and from neutron capture in the water reflector and moderator. LENS will use protons of two energies. Phase 1 will bombard the target with 7 MeV protons. Eventually, phase 2 will use 13 MeV protons. The Q value in this reaction is -1.85 MeV, so the product neutrons will have energies up to 5.15 and 11.15 MeV, respectively.

The goal of this project is to determine the flux and energy of the produced neutrons. This involves a three-fold task: first to learn how scintillation detectors work, second to model various detector schemes, and finally to design and construct a fast neutron detector. Fast neutrons have kinetic energies above 0.1 MeV. They are detected here through proton recoil in the (n, p) reaction on hydrogen. The moving proton is detectable in a scintillator.

2 Equipment

2.1 Scintillator Operation

General features of a scintillator are described below. In short, a scintillator is a type of detector which glows when charged particles pass through. The light output depends on the energy loss of incident charged particles.

2.1.1 Particle Interactions

When heavy charged particles (protons or alpha-particles) pass through a medium, they slow down due to Coulomb interaction with surrounding atoms. These interactions may stimulate the nearby atoms to become excited, or even ionize. Once these atoms de-excite, they emit light [1].

Electrons lose energy by Coulomb interaction similarly to the heavy charged particles. They also emanate bremsstrahlung (electromagnetic radiation) while decelerating rapidly near atomic nuclei. Again, de-excitation of excited atoms emits light [1].

Gamma interactions arise from three separate processes. *Photoelectric absorption* occurs when a gamma interacts with an absorbing atom and it completely disappears. In its place, an energetic photoelectron is ejected from one of the atom's bound orbits. This electron has all of the initial gamma's energy, neglecting binding energy. This effect is mostly found in crystalline scintillators (due to their high-Z materials). *Compton scattering* takes place when an incoming gamma scatters off an atomic electron in the absorbing material. The electron may absorb a portion of the gamma's energy depending on its deflection angle (see Eq. 1) and then be detected. Finally, *pair production* occurs whenever the gamma energy exceeds twice the rest mass of an electron. Sometimes when the gamma passes through the Coulomb field of a nucleus, it will disappear and an electron-positron pair will appear

in its place. The positron is eventually captured and annihilates, creating two new gammas, each with the rest energy of the positron (511 keV) [1].

2.1.2 Electronics

A scintillation detector consists of a scintillating material, a photomultiplier tube (PMT), and a base. The scintillating material emits small amounts of light, as described above. When an incident photon impinges upon the photocathode, one or more electrons are emitted by the photoelectric effect. They are accelerated toward the next dynode. A single electron incident on a dynode causes several electrons to be ejected from it. There are typically 12 dynodes in a PMT, and electrons are multiplied at each dynode in a cascade reaction. Between $10^7 - 10^{10}$ electrons will result from this reaction in 20-50 ns. This requires high voltages (HV) to operate. A voltage "ladder" is set up between the dynodes such that each potential difference is approximately equal. The voltage at each dynode is higher than the last. The electrons are thereby accelerated between two dynodes. The base holds the terminals for the electron pulses and HV for the voltage divider chain [2].

There are typically three terminals on the base of the scintillator: HV, Anode, and Dynode. The HV port is connected to the high voltage **of the polarity indicated** next to the port. The anode (the final dynode in the cascade chain) generates a strong signal which goes to various parts of the electronic setup. The dynode port corresponds to the first dynode in the cascade chain. It generates a much smaller, but faster signal. A typical HV setting is approximately 1500 volts for PMTs used with NaI and plastic scintillators. It is not uncommon to use a value as small as 700 volts or as large as 4500 volts.

2.2 Fast Electronics

To set up the detectors to acquire the recoiling proton spectrum, one uses various fast electronic modules. Each of these modules deals with the small signals from the detectors. Basic modules and characteristics are shown in Fig. 1 and described below.

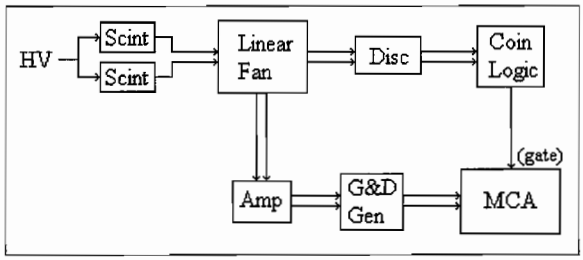

Figure 1: Basic electronic setup for a scintillator detector. Here, two scintillator spectra are analyzed in coincidence.

2.2.1 NIM and TTL Logic

Table 1: Logic Signals

Signal	Off Voltage (V)	On Voltage (V)
NIM	0	-0.8 to -1
TTL	0 to 0.7	1.5 to 5

Logic signals are digital "on"s and "off"s used for simple boolean logic in the fast electronics. These are short duration square waves used to tell fast electronics to function at a given time. For example: a counter will register a count for every square wave it receives.

There are two common logic signals in these electronics: NIM and TTL. NIM signals are **negative** signals which are less than 2 volts. More specifically, a voltage between -0.8 V and -1 V is considered a digital "1", while 0 V is considered to be a "0". NIM stands for Nuclear Instrument Modules. Logic signals from several crate modules (such as coincidence) are of this form [3].

TTL signals are **positive**, higher voltage signals. Voltages between 0 V and 0.7 V are a digital "0", while those between 1.5 V and 5 V are a "1". . TTL stands for Transistor-Transistor Logic.

2.2.2 Discriminators and Coincidence Logic

Discriminators send out a logic pulse when an input signal is above a certain threshold value, which may be adjusted. The width of the pulse may also be adjusted. Multiple copies of the input signal (produced either with a fan

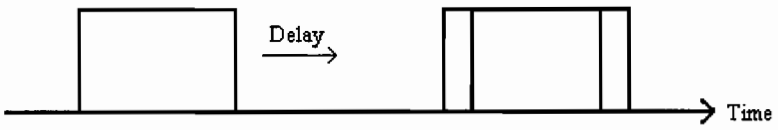

Figure 2: Delaying a logic pulse so that it overlaps with a later pulse from a separate source.

out, or just a T connector in the cabling) go to the discriminator and to a multichannel analyzer (MCA). The discriminator's pulse (square wave, logic signal) is sent to a gate on the MCA, telling the MCA to read the raw signal (wave with tail on end, data signal) when the pulse height is above the set threshold. This is useful for preventing background noise from accumulating.

Similarly, a coincidence logic module also sends out a pulse meant to trigger data analysis. If each detector has its own discriminator in a setup, then the pulses generated in the discriminators may go to a coincidence unit. When two or more of these signals arrive in an overlapping time, the coincidence unit fires a pulse of its own. Its pulse may also be used to trigger a multichannel analyzer to read data. This allows one to see several signals "in coincidence". The number of input pulses required to fire the coincidence module may be set on the module.

2.2.3 Amplifiers and Gate and Delay Generators

The signal from the detector is usually small, and must be amplified to be digitized and sent to the computer. An amplifier may increase the size of a pulse several times. The *pulse shaping* characteristic determines the length (in time) of the tail at the end of an amplified pulse. This should be short to avoid a new pulse adding to the tail of a previous pulse. Integration and differentiation time constants determine the overall shape of the pulse and tail. The signal-to-noise ratio is also dependent upon pulse shape. In most cases, optimum signal-to-noise is obtained when these time constants are equal [2].

One should always check output from an amplifier with an oscilloscope. Sometimes a large pulse will exceed an amplifier's maximum output, and some data will be lost. This is seen in the form of a wave that has a flat top on the oscilloscope.

Also of interest is the relative timing of the pulses with respect to each

other. This becomes important for coincidence logic, for example. The pulses received must overlap in time to be in coincidence. Sometimes though, depending on the situation, the signals will come several microseconds apart. To correct this, one may use a gate and delay generator (G&D) as shown in Fig. 2. These devices add adjustable delays to any signal. They convert negative signals to positive and also amplify. If one wants to convert NIM to an MCA acceptable signal, a G&D generator is a possible solution.

2.2.4 Multichannel Analyzer (MCA)

An MCA sorts incoming pulses according to pulse height and tallies them in corresponding channels in memory. A modern, computerized MCA is integrated with a computer for faster processing. An MCA will take any positive signals it receives between 0 and 10 volts. An analog to digital converter (ADC) within the MCA will digitize this voltage and assign it to a channel. A 0 V signal causes the lowest channel to register a count, while 10 V causes the highest channel to register a count. The *conversion gain* may be used to scale the voltage-to-channel assignment. Discriminators are usually used to prevent noise from overpopulating lower channels. Noise would cause the MCA to spend time collecting the noise and miss desired data.

Fig. 3 shows counts collected with a sodium-idodide (NaI) scintillator detecting a ^{137}Cs γ source. The channels here have been converted to energy values (more on this in the section on Spectral Analysis) [2]. This source has a single gamma peak at 662 keV, which appears distributed around a particular channel number.

Sometimes, there is a second port on the MCA to input a gate signal. This is where one would input a signal from a coincidence unit, for example. Configuring the software to use a signal from a gate will cause the MCA to only collect data when the gate receives a pulse.

More advanced MCA units may store all the data from each detector in a setup. This is sometimes preferred, since data storage is much cheaper than beam time. Data may later be analyzed via software as necessary: discriminators may be set within software, along with coincidence logic. Data are lost when hardware discriminators omit low energy points, but software discrimination only interprets stored data [4].

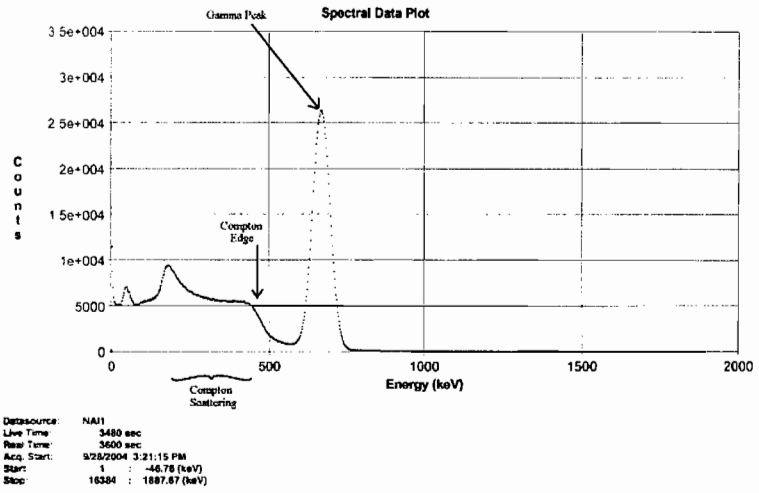

Figure 3: Energy Calibrated spectrum of ^{137}Cs on a 2 in^3 NaI scintillator. The large peak corresponds to 661.65 keV. One may also see the Compton edge, which is at 477.33 keV, given by Eq. 1.

2.3 Spectral Analysis

Software accompanying an MCA will sort the signals depending on the height of the pulse (the voltage of the signal). The sorted data is plotted, with pulse height along the horizontal axis and number of counts along the vertical axis. This plot is called the *pulse height spectrum.*

Calibrating the MCA is straight forward. Some radioactive isotopes, such as ^{137}Cs, have a single gamma peak of known energy. This energy may be set to the central channel (centroid) of the peak. Inputting several such peaks, accompanying software calibrates the spectrum. This calibration scales the channels to appropriate energies by estimating the light response of the detector by fitting the data (discussed in Sect. 4.4). After calibration, unknown sources may be placed near the detector and may be identified from the energies associated with the peaks. A calibrated spectrum is shown in Fig. 3.

Examining Fig. 3, one notices a large peak at 662 keV. This peak comes from gamma emission of the ^{137}Cs. The detector used here is NaI, which has a large photoelectric cross section. If the detector had been plastic, then this

peak would be absent. Compton scattering would be the main indication of the presence of ^{137}Cs when using a plastic scintillator.

The Compton edge (the energy cutoff point for Compton scattering) associated with a particular gamma peak may be found by using Eq. 1 [5]. Here, K_{max} yields the maximum energy that may be transferred to an electron in Compton scattering, and hence the Compton edge's position.

$$K_{max} = \frac{h\nu}{1 + \frac{1}{2\alpha}} < h\nu \quad (MeV) \tag{1}$$

with

$$\alpha = \frac{h\nu}{m_0 c^2} \tag{2}$$

Finally, one knows that $m_0 c^2 = 0.511$ MeV for an electron. This allows one to derive Eq. 3, where E_γ is the energy of the peak, and $E_{compton}$ is the energy of its associated Compton edge. The Compton edge denotes the maximum energy a recoiling electron may receive from the gamma.

$$E_{compton} = \frac{E_\gamma}{1 + \frac{511}{2E_\gamma}} \quad (keV) \tag{3}$$

Light response must also be calculated to generate an energy spectrum from a pulse height spectrum. The conversion of energy to light in a scintillator is usually a nonlinear process. dL/dx (fluorescence per unit length) depends upon energy, the type of charged particle, and the type of scintillator. The response of a plastic scintillator is well known for the energies of protons used here [6]. Light response is further described in Sect. 4.4.

3 Designing a Neutron Detector Scheme

The ideal detector would detect every neutron that passes through it and give its energy with high precision. This is not possible, since scintillators and proportional counters are not directly capable of detecting neutrons; neutron energy must first be transferred to a charged particle.

There are several reactions in which neutron energy is converted into charged particle movement. Used throughout this paper is the (n, p) reaction on hydrogen, where a neutron simply recoils off a proton, causing the proton to move. There are also common (n, α) reactions described below which produce a charged particle [7]. These are more common for thermal neutrons

with energy on the order of meV due to the reaction cross section's energy dependence.

$$n + {}^{10}B \longrightarrow {}^{7}Li^{*} + {}^{4}He + 2.3\,MeV \tag{4}$$

$${}^{7}Li^{*} \longrightarrow {}^{7}Li + \gamma\,(480keV) \tag{5}$$

$$n + {}^{6}Li \longrightarrow {}^{4}He + {}^{3}H + 4.64\,MeV \tag{6}$$

The following reaction is especially useful when used in a highly efficient ^{3}He proportional counter:

$${}^{3}He + n \longrightarrow {}^{1}H + {}^{3}H + 770\,keV \tag{7}$$

3.1 Details of Detector Selection

Neutron-proton scattering is the primary reaction discussed here. This is a process where a neutron displaces a proton with simple kinematics. If the neutron scatters from its path with angle ψ, then the proton recoils with energy

$$E_p = E_n \sin^2\psi \tag{8}$$

A series of detectors (scintillators and/or proportional counters) are likely to be used in future experiments. A thin detector in the front would ideally yield the energy loss $\triangle E$, while a thick detector further downstream would yield E. The front detector may also serve as a proton radiator.

Also considered is the possibility of using a thin proportional counter for the $\triangle E$ detector rather than a scintillator. A preferred arrangement with scintillators is to have the $\triangle E$ detector being the same thickness as the range of the fastest proton passing through it. This allows for protons from the entire first detector to interact with the next detector in the series. Unfortunately, this is impractical using plastic scintillators. A 10 MeV proton in plastic has a range of about a millimeter!

If instead, the $\triangle E$ detector is a proportional counter, then the lower stopping power will allow protons to pass through. A plastic proton radiator may be used to produce recoil protons in a setup involving proportional counters. Such a scheme is shown in Fig. 4. Placing all these detectors in

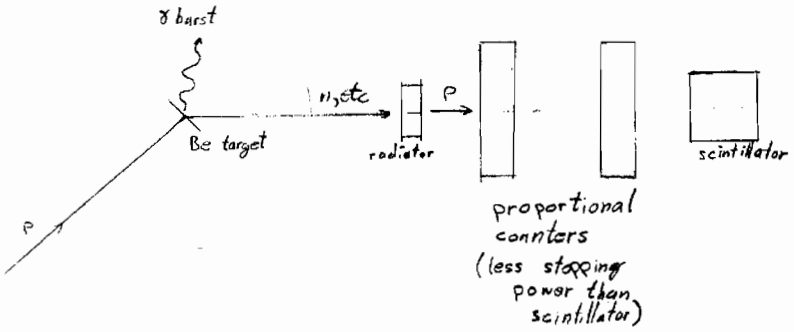

Figure 4: Sketch of possible detector arrangement.

coincidence would ensure that protons are coming from the proton radiator. This would aid in the reduction of background due to stray protons and neutrons.

3.2 Modelling Energy Loss

If one uses detectors in series, one must predict how much energy is lost by the recoil protons within each detector. One must also correlate this to the probability of a neutron colliding with a proton within the detector.

For example, it is described here how to find the theoretical proton stopping power of a plastic scintillator. One may use values from the PSTAR Database Program [8] to find a formula. The basis of the formula is the assumption that

$$R(T, \alpha, \beta) = \alpha(T)^{\beta} \tag{9}$$

Here, R is the proton range in g/cm^2, T is kinetic energy in MeV, and α and β are constants determined from the values from PSTAR. Fig. 5 shows the validity of this approximation. This relation may be rewritten to solve for T with an initial T_0, as shown in Eq. 10. In Eq. 10, x gives the distance traversed in the scintillator in g/cm^2.

$$T = (T_0^{\beta} - \frac{x}{\alpha})^{\frac{1}{\beta}} \tag{10}$$

α and β are found through Eq. 11 and Eq. 12 to be 0.00192 $g/cm^2/MeV^{\beta}$

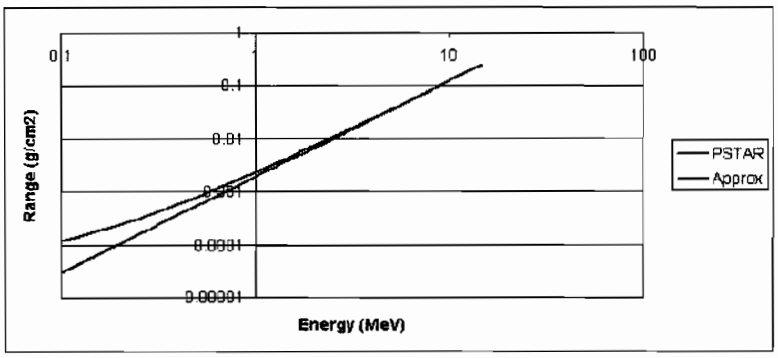

Figure 5: Log-log plot of proton range vs energy in a plastic scintillator. PSTAR values are compared to those produced by the approximation in Eq. 9 for α and β given in the text [8].

and 1.803 (an exponent without units). These are found using values for $T_1 = 1MeV$ and $T_2 = 10MeV$. The neutron energies here range from 0.1 MeV to 11 MeV, so this basis for the approximation is appropriate. Also, the maximum range of a proton in g/cm^2 is given by αT_0^{β}.

$$\beta = \frac{ln\, R_1 - ln\, R_2}{ln\, T_1 - ln\, T_2} \tag{11}$$

$$\alpha = \frac{R_1}{T_1^{\beta}} \tag{12}$$

The results of this equation are shown in Fig. 6. In Fig. 6, it is assumed that protons are entering the scintillator with energies of 5.4 MeV and 11.5 MeV, as created by the neutrons of similar energies hitting a proton radiator. These energies are near to the maximum neutron energy in each phase of LENS. The main finding of this is that the proton kinetic energy is zero after travelling 0.39 mm and 1.52 mm, respectively. From this, one concludes that scintillator detectors in series are impractical.

Again, it is noted that this method models *actual* energy lost, not the light emission. The light emission in a scintillator due to protons is nonlinear and is a function of dE/dx for the proton. This is further described in Sect. 4.4

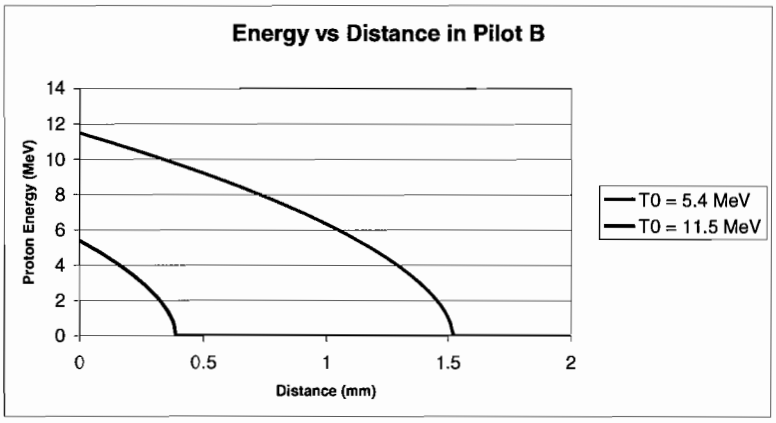

Figure 6: Approximate proton energy as a function of distance traversed in a plastic scintillator. This uses Eq. 10.

3.3 Probability of Neutron/Proton Collision

The probability of a neutron colliding with a proton must be calculated before designing a detector scheme. Proton radiators are more likely to produce protons with increasing radiator thickness. However, protons will lose energy within the radiator. Energy loss must again be taken into account when choosing the radiator. Eq. 13 gives the probability of creating protons within a plastic scintillator.

$$N_p = \frac{n_H \sigma_H}{n_H \sigma_H + n_C \sigma_C} \{1 - \exp[-(n_H \sigma_H + n_C \sigma_C) d]\} \tag{13}$$

In Eq. 13, the n's give the number of $atoms/cm^3$. The σ's are the associated neutron-proton elastic cross sections, which are in cm^2 here. The σ's are energy dependent, and are described below. Finally, d is the distance traversed in the plastic scintillator in cm.

3.3.1 Finding the Molecular Densities

From PSTAR [8], one knows the density of a plastic (polystyrene, $C_6H_5CH = CH_2$ [9]) scintillator is 1.032 g/cm^3. One also finds that 91.54% by weight is carbon, while the other 8.451% is hydrogen. This means C molecules take up 0.9447 g/cm^3 while H takes up 0.08721 g/cm^3. Using Avogadro's

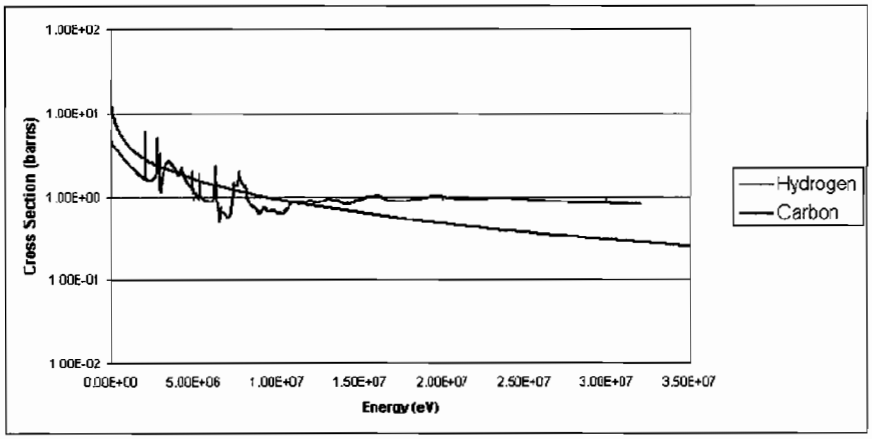

Figure 7: Cross sections of Hydrogen and Carbon atoms for neutron-proton elastic scattering.

number, one finds that there are $4.737 \times 10^{22}\ atoms/cm^3$ of C, and $5.210 \times 10^{22}\ atoms/cm^3$ of H.

3.3.2 Cross Sections

One may find values of the cross sections by looking at the T-2 Nuclear Information Service [10]. Fig. 7 plots the numerical values of the cross section found for neutron-proton elastic scattering for hydrogen as a function of neutron energy. Carbon (^{12}C) has a more complicated plot, also shown in Fig. 7. It is more complicated due to increased complexity of the nucleus. The units of cross section are typically given in barns, where $1\ barn = 1 \times 10^{-24}\ cm^2$.

The many resonances in the carbon cross sections cause problems when inputting them later. These problems may be fixed using Riemann sums. In these sums, the cross sections are multiplied by half the energy to the adjacent cross sections. These products are added together. This is repeated for cross sections $\sigma(E_i)$ spanning each bin of size 0.1 MeV. This technique approximates the exact integral in Eq. 14 as Eq. 15. Upon dividing by the bin width of 0.1 MeV, one finds the effective average cross section within each bin. In these equations, a and b correspond to the lower and upper energies of the bin.

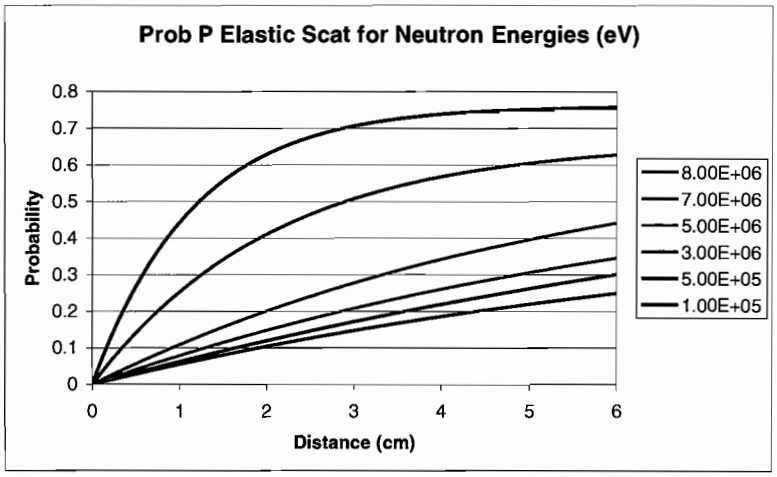

Figure 8: Probability of proton recoil in polyethylene for a neutron of given energy. This results from Eq. 13

$$\sigma_{ave} = \frac{1}{b-a}\int_a^b \sigma(E)dE \tag{14}$$

$$\sigma_{ave} \approx \frac{1}{b-a}\sum_i \sigma(E_i)\triangle E_i \tag{15}$$

3.3.3 Resulting Probability

Examining Fig. 8, one notices that the thickness of a proton radiator would have to be on the order of a few cm in order to have most neutrons collide with protons. However, one must consider the energy loss shown in Fig. 6. The plastic scintillator is also the basis for this energy loss diagram, which means that protons created in this proton radiator will stop almost immediately! A reasonable compromise must be found between proton production rate and energy loss.

Also notice how the higher energy neutrons seem to interact with probability increasing linearly with distance. This is due to the low cross section at higher energies. One may see this by taking a Taylor expansion of an equation similar to Eq. 13.

$$1 - e^{-\sigma d} = 1 - \left(1 - \sigma d + \frac{(\sigma d)^2}{2!} - ...\right) \approx \sigma d \quad \sigma d \ll 1 \tag{16}$$

4 Monte Carlo Model

To plan an appropriate series of detectors for fast neutron detection, a Monte Carlo program in *Fortran 77* was written to predict particle interactions.

The Monte Carlo program combines the known probabilities in the problem, then uses a random number generator to simulate the physics of many individual particles. The model here combines (n, p) elastic scattering cross sections of carbon and hydrogen, abundances of carbon and hydrogen in the material, thickness of material, location of (n, p) reaction in material, energy loss of proton after (n, p) reaction, and the angle of the scattered proton. Secondary scattering and light response are also modelled.

Using these simulation results, one may tabulate data to create an energy spectrum. This theoretical spectrum may easily be compared to an actual spectrum. Later, other situations may be modelled. This allows for the fast simulation of experiments that could take days to set up and execute. Overall detection efficiency may also be estimated. The original motivation behind this simulation was to explore the practicality of having an array of scintillators for fast neutron detection.

The scintillator model uses experimental data to model the characteristics of a standard plastic scintillator (also known as Pilot B) [8]. A convenient feature of the plastic scintillator is that it is an efficient proton radiator. It is comprised of CH_2 and hydrogen is abundant. Modelling a second detector (not necessarily a scintillator) may use this model as a proton radiator. Energies of escaping protons with certain scattering angles are easily stored for later use.

4.1 Random Number Generation

Before discussion of a model, one must take a moment to consider random number generators (RNGs). These are key to the Monte Carlo concept. Computers may only generate *pseudo* random numbers. This means that the computer uses an algorithm with an extremely long period, which seems to be random. To ensure a new set of random numbers each time the program is run, one uses the TIME function as a seed. The TIME function returns a

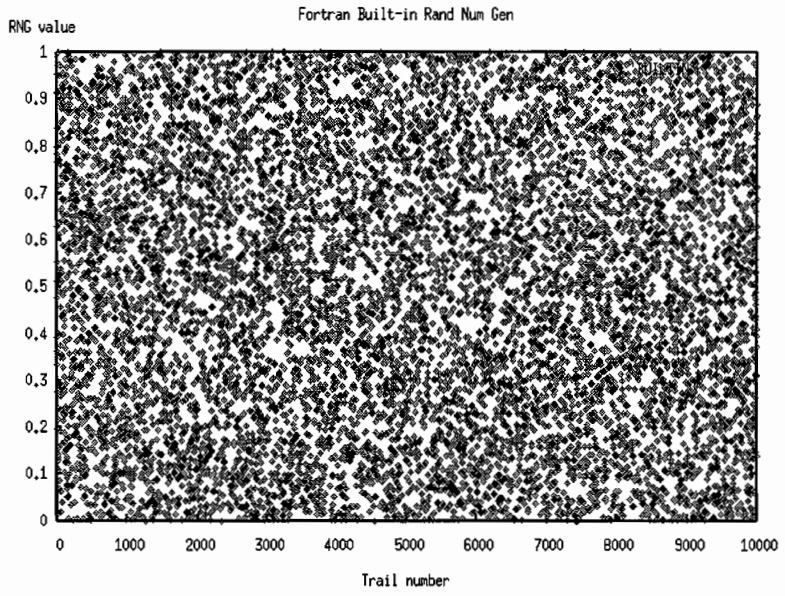

Figure 9: Random numbers produced by built in RAND function.

numerical value based on the date and time according to the system clock. This gives the program a new starting point each time the program is executed. Fortran's built in RAND function produces Fig. 9. No apparent patterns are present, indicating an acceptable choice for an RNG.

4.2 Neutron Spectrum

The first step of the program is to determine an incident neutron energy. To ensure program accuracy, one uses known experimental neutron spectra from Am-Be [11]and Pu-Be [12] sources to choose a random neutron energy between 0.1 and 11 MeV. Tallying many such random energies regenerates the original spectra. Previous studies have determined the neutron flux from these standard sources, and the results are shown in Figs. 10 and 11. These data are entered into bins of size 0.1 MeV. The results of the program are later compared to scintillator data from similar sources.

The function AMBESPEC or PUBESPEC is called, and returns a neutron energy. Two random numbers are generated: a neutron energy and a test value. If the test value falls below the associated spectrum, then the neutron

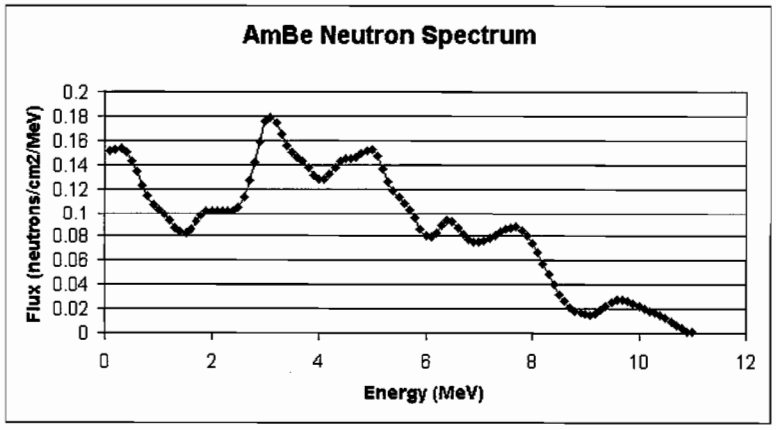

Figure 10: Experimentally determined neutron flux from an Am-Be source. (Kluge and Weise 1982) [11]

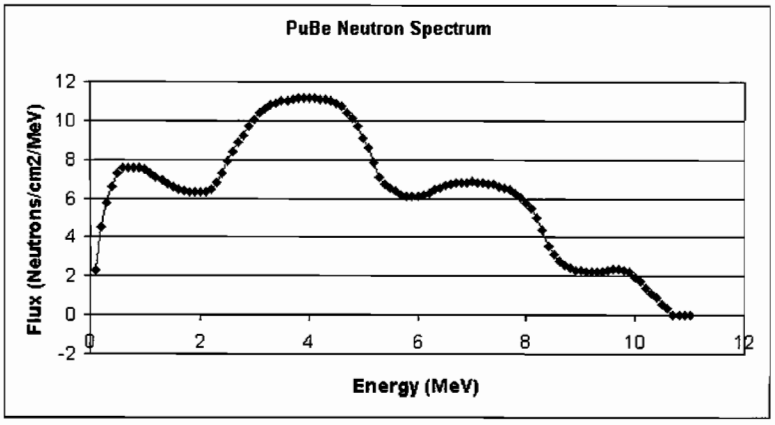

Figure 11: Experimentally determined neutron flux from a Pu-Be source. (L. Stewart 1954) [12]

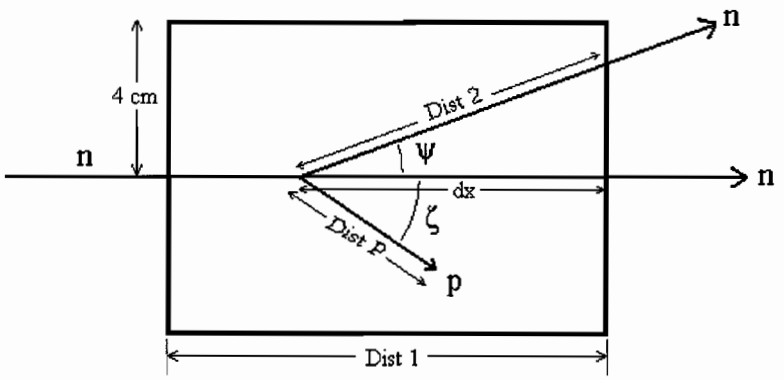

Figure 12: Proton recoil geometry for a cylindrical plastic scintillator of radius 4 cm. Neutrons enter at the cylinder's center from the left. The point of recoil is randomly distributed along the neutron path.

energy is returned. If the test value is above the spectrum, then the process restarts. This in itself is a Monte Carlo process.

4.3 Geometry

4.3.1 Primary Proton Recoil

Most light generated in a proton recoil detector results from the primary (n, p) reaction on hydrogen. To approximate a detector, one assumes a cylindrical detector of radius 4 *cm* and length *Dist* 1. One further assumes that all neutrons enter along the axial center of the detector. When an incident neutron successfully hits a hydrogen atom, a recoil proton is produced at an angle ζ with respect to the incident neutron path. This is shown in Fig. 12. The angle in the center of mass frame of the neutron is predicted from experimental results [10]. Since a neutron and proton are nearly equal in mass, this may be divided by 2 to find the angle ψ. Then, since $\zeta + \psi = 90°$, one may find the maximum *Dist P* to be given by Eq. 17. The maximum range of the proton will never allow it to reach the 4 *cm* edge of the cylinder, so the distance it travels is only considered to the rear. In Eq. 17, *RN* is a random number between 0 and 1, used to determine the value *dx*.

$$Dist\ P = \frac{Dist\ 1 \times RN}{\cos(90° - \psi)} \tag{17}$$

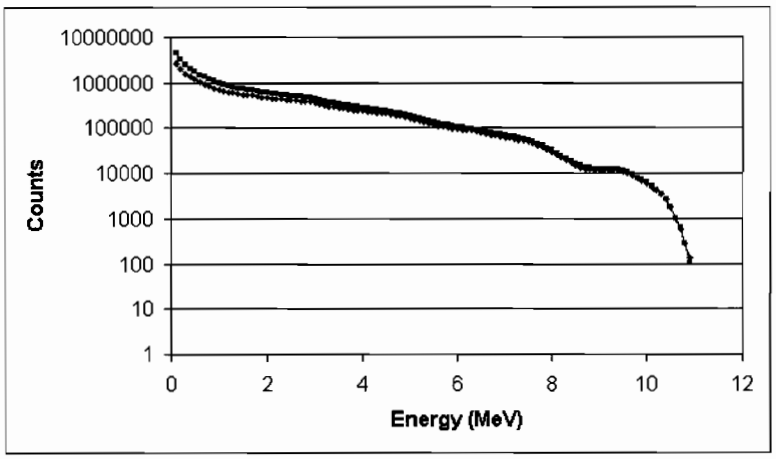

Figure 13: Resulting energy loss histogram for the Am-Be source, as predicted by simulation. The green line shows the result with secondary scattering, the blue without.

Eq. 17 is a non-relativistic approximation for these collisions [13]. Since the maximum neutron energy = 11 MeV $\ll$ 931 MeV, this approximation holds. As mentioned earlier, the energy of the proton after such a collision is given by Eq. 8.

Once Eqs. 17 and 8 are used for a given angle, neutron energy, and dx, Eq. 10 may predict the remaining energy in the proton after it has reached the edge of the scintillator. The proton stops after traversing a few millimeters in the scintillator. If the proton range is smaller than *Dist P*, then energy for the exiting proton is zero. By subtracting the remaining energy from the initial proton energy predicted by Eq. 8, the total energy loss is determined. This may then be related to light output.

4.3.2 Secondary Scatter

Secondary scatter makes a small, noticeable effect at lower energies in the spectrum (see Fig. 13). It occurs when a neutron scatters from a hydrogen atom *after* it originally scatters from a hydrogen or carbon atom. These secondary scatters are the second largest source of light generated in the detector. Other sources of light are present, but may be considered negligible [1].

Again, notice the geometry depicted in Fig. 12. For primary scattering from a hydrogen atom, the distance of travel for the deflected neutron is given by

$$Dist\ 2 = \frac{Dist\ 1 \times RN}{\cos\psi} \tag{18}$$

if $dx \times \tan\psi < 4.0\ cm$, otherwise it is given by

$$Dist\ 2 = \frac{4.0\ cm}{\cos\psi} \tag{19}$$

Eq. 19 is required in case the neutron exits from the edge of the cylindrical detector. The 4 *cm* term results from the radius of the detector, and may be changed. Meanwhile, the new neutron energy is given by

$$E_{n2} = E_n\ \cos^2\psi \tag{20}$$

From here, the process for primary scattering is repeated with the new values of *Dist* 2 and E_{n2} replacing *Dist* 1 and E_n. This is an approximation that assumes the new recoiling proton takes on a path similar to the neutron, and reaches the wall in the same distance as the neutron. The proton actually has a direction within a cone around the path of the neutron. Without the approximation, another dimension would be needed to predict a small effect. Fig. 14 shows this situation.

In Fig. 14, the brown cylinders correspond to the path of the neutron through the green detector. The blue cylinder shows the short distance travelled by a proton. Finally, the blue cone shows possible paths of the proton produced in secondary scatter. The path of the proton would lie on the outer edge of this cone, where the angle of the cone is determined in the same way as the original ζ from Fig. 12. The approximation deviates from actual path length when the cone lies partly outside of the green detector.

The probability of a neutron scatter from a carbon atom in the ^{12}C(n, n)^{12}C reaction is given by Eq. 13, except with carbon coefficients in the numerator. To find the scattering angle of the neutron, one uses the same arguments as above, with the additional condition that angles ψ greater than 90° are subtracted from 180°. This subtraction works because of the forward/backward symmetry of the detector. With (n, p) reactions on hydrogen, the neutron has been confined to forward scattering by the kinematics. Scattering from a heavy carbon atom, however, allows the neutron to go in any direction.

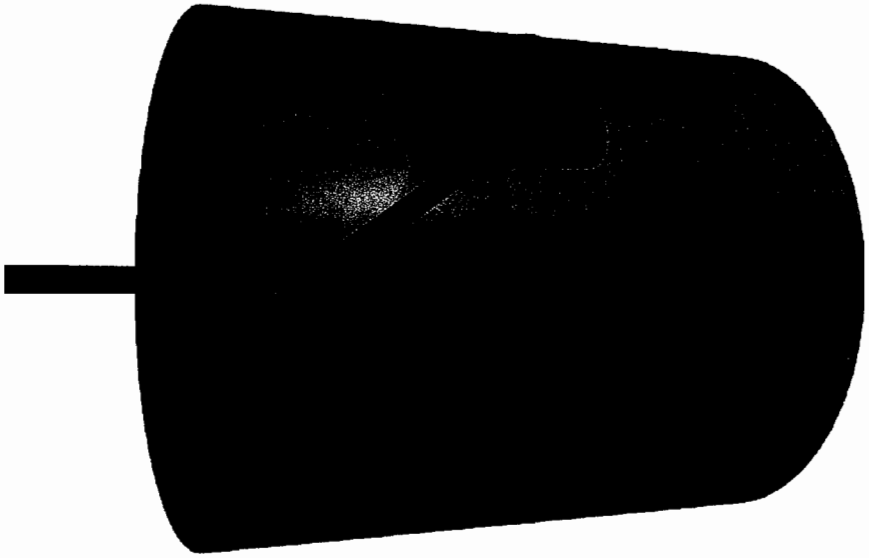

Figure 14: The blue cone here indicates possible paths for the proton to take in secondary scattering.

The energy of the carbon scattered neutron is given by a more complicated function since the masses are no longer equal, as shown in Eq. 21 [13]. This type of secondary scatter contributes about the same amount of light to the final spectrum as secondary scattering from hydrogen. Carbon and hydrogen scattering occur with similar probability due to their near cross sections (Fig. 7) and abundances. Approximately 40% of the light results from multiple scatter at the lowest energies, while no additional light is generated at the highest energies. On a log scale, even 40% makes little difference, as shown in Fig. 13.

$$E_{n2} = E_n \frac{m_n^2}{(m_n + m_C)^2} \left[\cos\psi + \sqrt{\left(\frac{m_C}{m_n}\right)^2 - \sin^2\psi} \right]^2 \tag{21}$$

4.4 Light Response

The final step of the program is to spread out the energy loss histogram as it would appear in the form of light. This step also uses experimental results for studies involving recoiling protons in plastic scintillators [6]. An equation

relating light output to proton stopping power is provided in Eq. 22. It is assumed that recoiling carbon atoms emit a negligible amount of light.

$$\frac{dL}{dx} = \frac{S\frac{dE}{dx}}{1 + kB\frac{dE}{dx} + C\left(\frac{dE}{dx}\right)^2} \tag{22}$$

Table 2: Eq. 22 Coefficient List for Recoil Protons in a Plastic Scintillator

Variable	Meaning	Value and Units
$\frac{dL}{dx}$	Fluorescent light emitted per unit path	$cm^2\,g^{-1}$
$\frac{dE}{dx}$	Stopping power of scintillator	MeV $cm^2\,g^{-1}$
S	Scintillation efficiency	2232 (Arb. Units)
kB	Fitting constant 1	$1.29 \times 10^{-2}\,g\,cm^{-2}\,MeV^{-1}$
C	Fitting constant 2	$1.05 \times 10^{-5}\,g^2\,cm^{-4}\,MeV^{-2}$

Table 2 lists the variables and constants in Eq. 22 describing a plastic scintillator. One may integrate Eq. 22 using a Riemann sum over the values of $\frac{dE}{dx}$ (similar to Eq. 15). This will yield L for any energy E lost. Using a ratio of L to E for each of the 110 energy bins in the program, the energy loss spectrum is transformed into a light spectrum. This essentially squeezes the left side of the histogram together, while the right is spread out. Fig. 15 shows light output as a function of pulse energy. Fitting this curve shows that light response of a plastic scintillator is proportional to proton energy loss to the 3/2 power.

5 Detection of Neutrons

5.1 Derivative Approximation Method

An interesting mathematical approach may be taken to approximate a neutron flux from a given energy spectrum. It relies on the assumption that neutron scattering is isotropic. Angular distributions from T-2 show variance on the order of 3%, justifying this assumption [10]. This distribution is shown in Fig. 16, where larger angles are slightly favored. One begins the approximation by defining the proton energy spectrum with

$$P(\varepsilon) = \int_0^\infty \phi(\varepsilon_n) E(\varepsilon_n) f(\varepsilon_n, \varepsilon)\, d\varepsilon_n \tag{23}$$

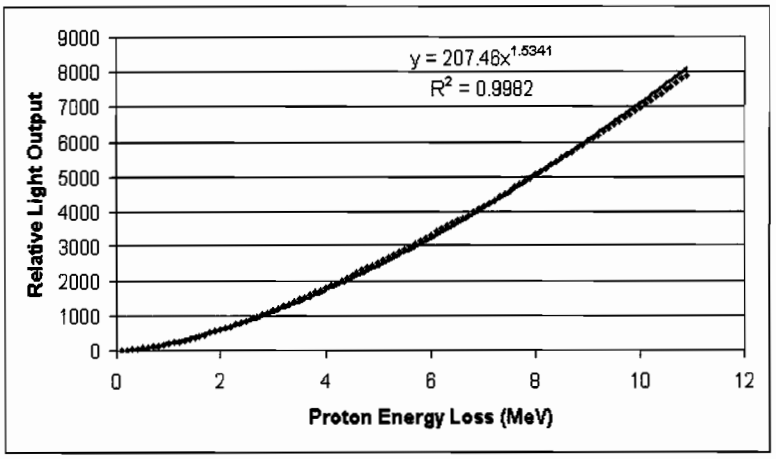

Figure 15: Relative light output vs proton energy loss in a plastic scintillator. This spans the range of used neutron energies and results from Eq. 22 [6].

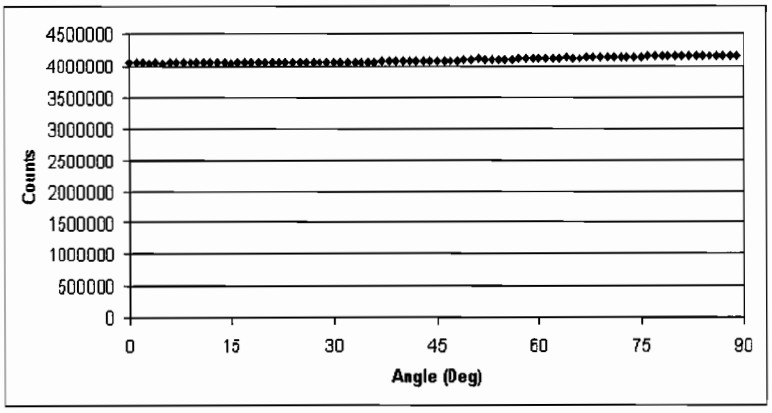

Figure 16: Histogram of neutron scattering angles (in the center of mass frame) generated in the Monte Carlo program. This angular distribution is obtained using data from T-2. [10]

In Eq. 23, P gives the probability of registering a count as a function of proton energy ε, ϕ gives the neutron flux as a function of neutron energy ε_n, and E gives the detection efficiency (probability of (n, p) reaction) for a given neutron energy. Finally, f gives the probability of generating a proton of a given energy based on an isotropic distribution of Eq. 8. Since all proton energies up to the neutron energy are equally likely in an isotropic distribution, f may be written as

$$\begin{aligned} f(\varepsilon_n, \varepsilon) &= \frac{1}{\varepsilon_n} \quad \varepsilon < \varepsilon_n \\ &= 0 \quad otherwise \end{aligned} \tag{24}$$

By inserting Eq. 24 into Eq. 23, one may rewrite this as

$$P(\varepsilon) = \int_{\varepsilon}^{\infty} \frac{\phi(\varepsilon_n)E(\varepsilon_n)}{\varepsilon_n} d\varepsilon_n = 1 - \int_{0}^{\varepsilon} \frac{\phi(\varepsilon_n)E(\varepsilon_n)}{\varepsilon_n} d\varepsilon_n \tag{25}$$

Taking the derivative of this, one finds

$$\frac{dP(\varepsilon)}{d\varepsilon} = -\frac{\phi(\varepsilon)E(\varepsilon)}{\varepsilon} \tag{26}$$

Finally, this is rewritten to produce the flux:

$$\phi(\varepsilon) = -\frac{\varepsilon}{E(\varepsilon)} \frac{dP(\varepsilon)}{d\varepsilon} \tag{27}$$

Eq. 27 shows that one may find the neutron flux incident on a detector simply by multiplying the derivative of the spectrum by the energy, then dividing by the detection efficiency. This reproduces major features of the flux, as shown in Figs. 19 and 22. Problems arise from the low statistics of the experimental spectrum, however. A derivative may only be approximated for the counts in each channel, for a finite number of channels.

5.2 Am-Be Source

Using the Monte Carlo techniques discussed above, Fig. 17 shows the theoretical spectrum of recoil protons in a plastic scintillator from an Am-Be source. This uses the neutron flux in Fig. 10 for a basis. The theoretical light response produces the red line in Fig. 18.

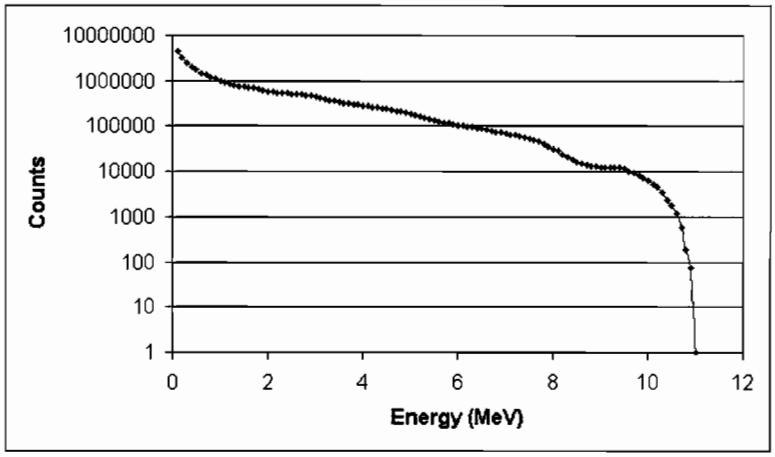

Figure 17: Expected scintillator energy loss histogram from Am-Be source, resulting from simulation.

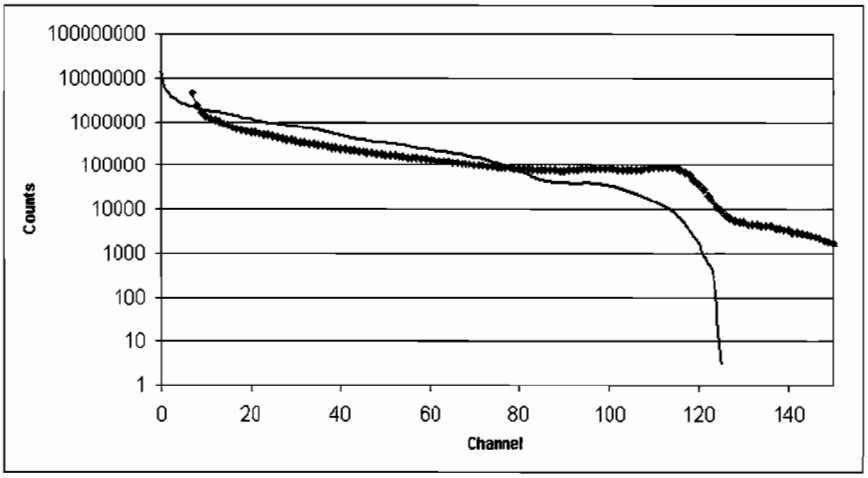

Figure 18: The red line is the light histogram expected from the Am-Be source, obtained by applying Eq. 22 to Fig. 17. The blue points are experimental data from a 2"x3"x4" plastic scintillator with lower channels omitted due to discriminator settings.

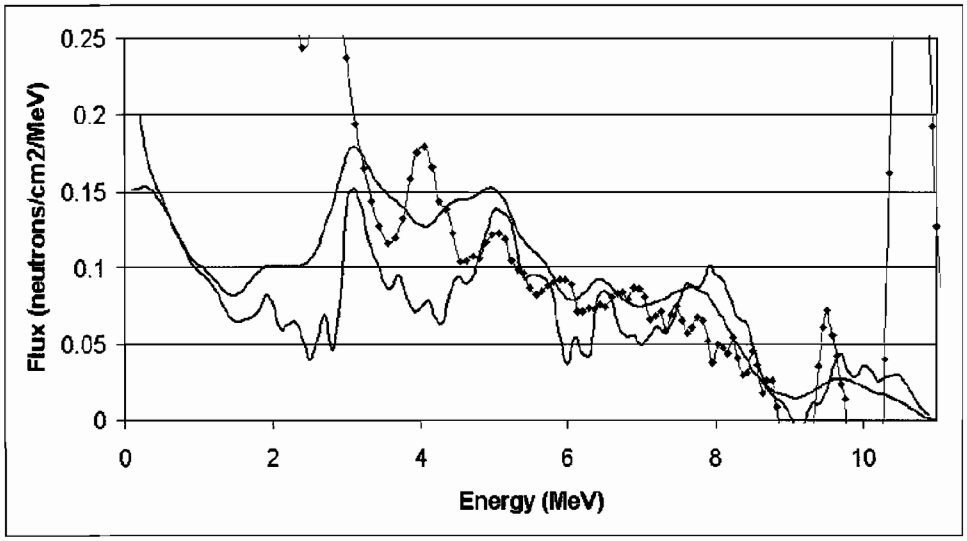

Figure 19: The red line is produced by applying Eq. 27 to the simulation in Fig. 17. This red line approximates the Am-Be spectrum (green line). The dotted blue line results from unfolding the experimental data in Fig. 18.

The theoretical spectrum in Fig. 18 may be compared to an experimental one. The theoretical spectrum has been vertically scaled to match the experimental data. Channel assignment of the theoretical data uses the light relation discussed in Sect. 4.4. Assignment of a channel to the 11 MeV maximum neutron energy is challenging. It is easier through use of the derivative method.

For a check of model accuracy, the derivative of the energy loss histogram is taken. Applying Eq. 27 to the data of Fig. 17, one produces the red line in Fig. 19. Also in Fig. 19, the green line shows the initial flux input into the simulation [11]. Other data are scaled to align with this initial flux.

The dotted blue line in Fig. 19 results from application of both light response and the derivative method to experimental data. By examining Figs. 18 and 19, one may choose which channel most likely corresponds to the maximum neutron energy. Here, channel 125 is decided to be equivalent to 11 MeV proton energy loss. This is required to fit the theoretical spectrum to the experimental data.

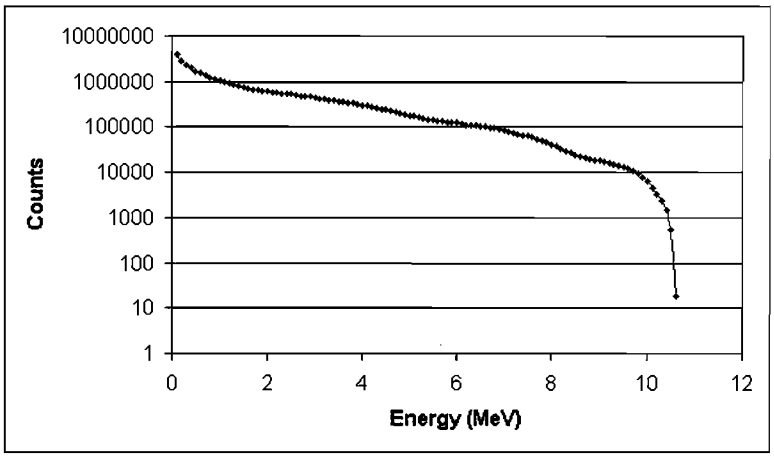

Figure 20: Expected scintillator energy loss histogram from Pu-Be source, produced by simulation.

5.3 Pu-Be Source

The same situation occurs when modelling the Pu-Be source. Energy loss is given by Fig. 20, using the neutron flux in Fig. 11. Fig. 21 compares the theoretical light output to the experimental result. Differences in these curves are believed to be caused by paraffin shielding surrounding the Pu-Be.

Finally, the derivative of the energy loss is shown in Fig. 22. The red line reproduces the source spectrum (green) quite well. When one applies the light relation and derivative method to experimental data in Fig. 21, the blue line is produced in Fig. 22. This seems to be inaccurate between 2 and 7 MeV, which correspond to channels 140 and 950. In Fig. 21, the pulse height spectrum between these channels seems relatively flat, but still similar to simulation. This demonstrates the criticality of an accurate model to successfully unfold a spectrum.

5.4 Sources of Discrepancy

The Monte Carlo results are similar to the experimental data, but there are differences. Perhaps the largest source of error comes from the simplification of geometry in the problem.

It is assumed that the detector is cylindrical and that all the neutrons

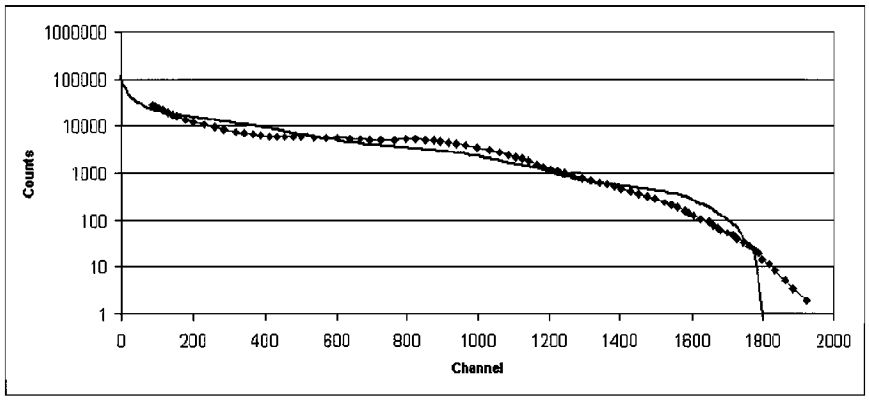

Figure 21: Experimental data from a plastic scintillator near a Pu-Be source. This source is surrounded by paraffin, except for a narrow tube (approximately 0.5 meters long) leading to the scintillator. The exposure time is 5 minutes. The red line results from Monte Carlo simulation.

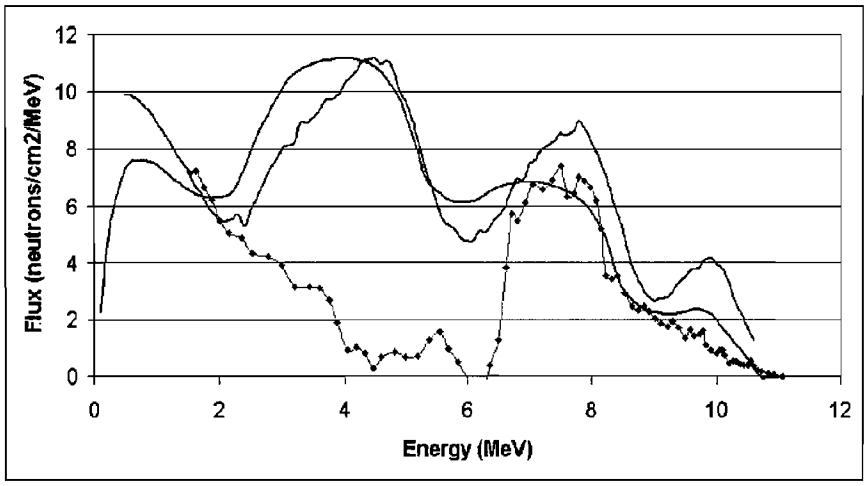

Figure 22: The red line is produced by applying Eq. 27 to the simulation in Fig. 20. This red line approximates the Pu-Be spectrum in green. The blue results from unfolding the data in Fig. 21.

enter along its central axis. This program has been written primarily to simulate spectra from LENS. For a long beam pipe, narrow in diameter compared to the scintillator, this is a fair assumption. Experimental data shown here for program testing do not fit these conditions.

The detector in each case is placed closely to a small source. This allows neutrons to pass through the scintillator at any path from the source, not just along the central axis. In the future, it may be worthwhile to place a mixture of paraffin and cadmium shielding around the detector to force neutrons to come from a common direction.

Also, the experimental spectra acquired in Figs. 18 and 21 were taken using different plastic scintillators. Since they diverge from simulation in different ways, one may deduce that different scintillators behave differently. Alternatively, the paraffin shielding around the Pu-Be source may have corrupted the data in Fig. 21 (due to neutron scatter from the shielding). This effect may cause the simplification of geometry through shielding to be a more challenging problem.

6 Conclusions

The Monte Carlo program predicts spectra that match experimental data quite well. One may see the overall process of the simulation in Fig. 23 (after conclusions). The next step is to perform further experiments to make these match more completely. By shielding the detector with layers of paraffin and cadmium in a future experiment, the geometry should simplify and sources of error will be reduced. Also, placing the plastic scintillator in a proton beam of known energy would allow for a more precise channel to energy calibration. This will allow for easier, more accurate interpretation of experimental data.

Once the simulation output matches the data satisfactorily, it will be time to use the scintillator and program to deduce the neutron flux from LENS. The goal of this Monte Carlo program has been to *fold* a neutron flux to find a spectrum, but one would like to *unfold* a spectrum to find a neutron flux. The first step in this process is to acquire experimental data with good statistics. The light relation in Fig. 15 will be used to convert the detected light to energy loss in the detector. This new energy loss spectrum can then be manipulated.

To a rough approximation, the derivative may be taken of the energy loss spectrum (as in Fig. 19 and Fig. 22) to see the general features of the neutron

flux. This, however, is insufficient for finding an accurate distribution. If the Monte Carlo program correctly describes all features of the detector, it may produce a far more accurate spectrum. One could input an experimental spectrum, then the source neutron flux may be adjusted over several runs until the output matches the given data.

7 Acknowledgements

I would like to thank Prof. Hermann Nann for giving me the opportunity to research low energy neutrons with him. Also, I thank Chris Lavelle for spending much time to help me get started with this research. Finally, I thank Prof. Hans-Otto Meyer for giving me the chance to study neutrons while in his modern lab course, and continuing to help me afterwards.

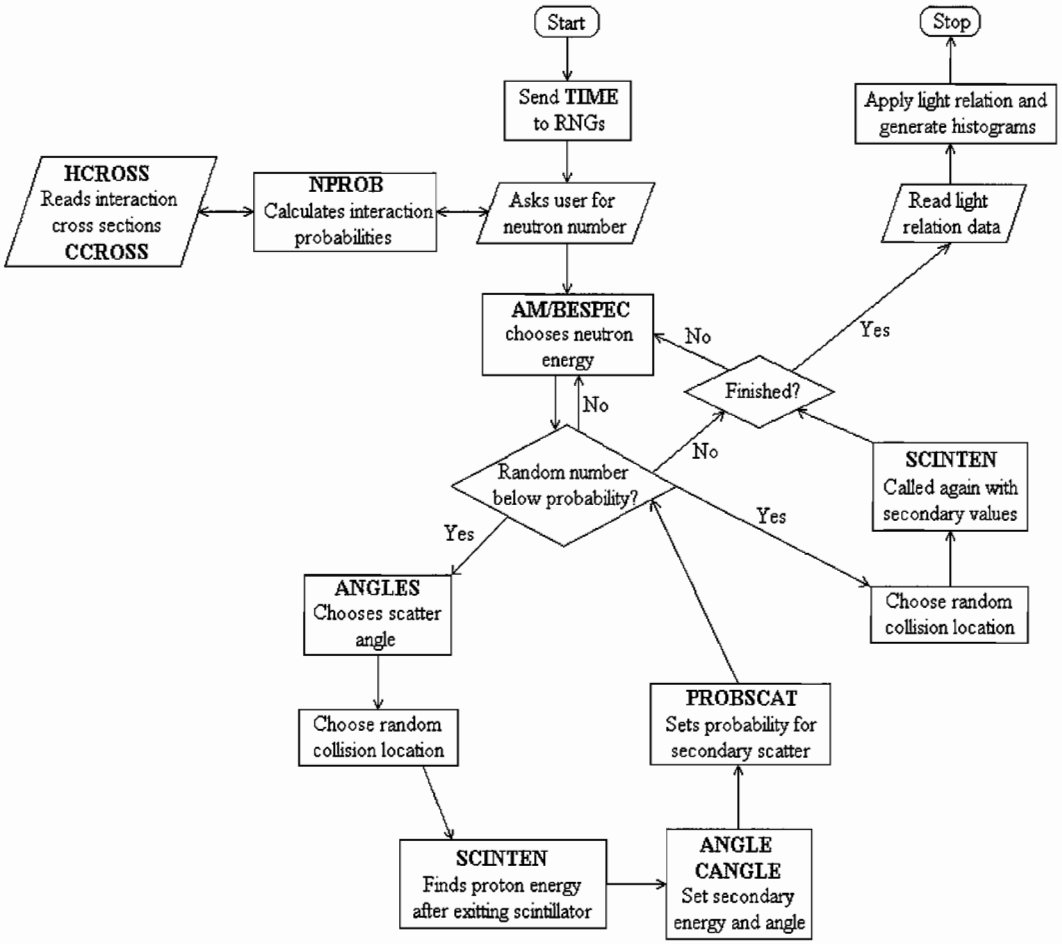

Figure 23: Flow chart for the Monte Carlo program described in this paper.

References

[1] Knoll, G. F. (1979). *Radiation Detection and Measurement.* New York, USA: John Wiley & Sons.

[2] Leo, W. R. (1994). *Techniques for Nuclear and Particle Physics Experiments: A How-to Approach* (2nd edition) Heidelberg, Germany: Springer-Verlag.

[3] Horowitz, P. & Hill, W. (2001). *The Art of Electronics* (2nd edition). New York, USA: Cambridge University Press.

[4] CERN. *PAW – Physics Analysis Workstation* [Program]. URL
`http://wwwasd.web.cern.ch/wwwasd/paw/`

[5] Preston, D. W. and Dietz, E. R. (1991). Nuclear Physics: Interaction of Gamma Rays with Matter. *The Art of Experimental Physics* (p. 321). New York, USA: John Wiley & Sons.

[6] Craun, R. L. & Smith, D. L. (1970). *Nuclear Instruments and Methods* (Vol. 80, pp. 239-244).

[7] (1960). Marion, J. B. and J. L. Fowler (Eds.), *Monographs and Texts in Physics and Astronomy Volume IV: Fast Neutron Physics Part I.* New York, USA: Interscience Publishing, Inc.

[8] NIST (2004). *NIST PSTAR Database Program* [Website]. URL
`http://physics.nist.gov/PhysRefData/Star/Text/PSTAR.html`

[9] Groom, D. E. (2002). Chapter 6: Atomic and Nuclear Properties of Materials. *Physical Review D: Particles and Fields* (1 July 2002, Vol. 66, pp. 84-85). Melville, USA: The American Physical Society.

[10] (2001). T-2 Nuclear Information Service. [WWW Page]. URL
`http://t2.lanl.gov/`

[11] Kluge, H. & Weise, K. (1982). The Neutron Energy Spectrum of a ^{241}Am-Be(α,n) Source and Resulting Mean Fluence to Dose Equivalent Conversion Factors, **Radiation Protection Dosimetry** (Volume 2, Number 2, pp. 85-93).

[12] Stewart, L. (1955). Neutron Spectrum and Absolute Yield of a Plutonium-Beryllium Source, **Physical Review** (Volume 98, Number 3, pp. 740-743).

[13] Thornton, S. T. & Marion, J. B. (2004). Dynamics of a System of Particles, *Classical Dynamics of Particles and Systems* (5th edition, pp. 345-354). Belmont, CA, USA: Brooks/Cole–Thomson Learning.

```
      PROGRAM CHAMB
C Monte Carlo simulation of neutron behavior
C in a plastic scintillator.
C As written, this assumes the neutrons 'disappear'
C after the first couple interactions.

C This variant should model a standard Am-Be or Pu-Be source.

C Updated:  May 16, 2005
C Author :  Jonathan Horton


C Declarations
      INTEGER TRIES, SUCCESS, PNEXT, ESORT(110)
      INTEGER ELOSS(110), EIN(110), NEUOUT(110), ENEU
      REAL DIST1, DIST, TANG, DX, TELOST, EREM, NPR
      DATA TELOST /0.0/, PNEXT /0/, ESORT /110 * 0/
      DATA ELOSS /110 * 0/, EIN /110 * 0/
      PARAMETER(DIST1 = 5.08) ! 2" Detector, may change
      DATA NEUOUT /110 * 0/
      REAL PROBS(110), PROBC(110), CHANCE, NPTOT, NEXTDIST
      INTEGER QUEN(1100)
      DATA QUEN /1100 * 0/
      REAL DX2, DIST2P, TANG2
      REAL MH, MC
      PARAMETER (MN = 939.6, MC = 11188.0)

C Starts up the random number generator using the
C system clock for a seed.
      IDUM = -TIME()
C Starts alternate random number generator...
      dummy = RAND(TIME())

C Stores probabilities of 1st hydrogren interaction
      OPEN(UNIT = 2, FILE = 'TOTAL')
C Energy tally for escaping protons with given angle
      OPEN(UNIT = 3, FILE = 'EOUT')
C Total energy lost in scintillator (no quenching!)
      OPEN(UNIT = 4, FILE = 'ELOSS')
C stores signal in first scint for protons hitting 2nd scint
      OPEN(UNIT = 8, FILE = 'EIN')
C stores spectrum of interacting neutrons
      OPEN(UNIT = 10, FILE = 'NEUOUT')

C User sets number of trials....
      PRINT *
      PRINT *, 'Am/Pu-Be spectrum simulation'
      PRINT *, 'How many neutrons to simulate?'
      READ *, TRIES

C Calculates all probabilities of first collision and stores them
C to speed up the program.
      CALL NPROB(DIST1, PROBS, PROBC)

      SUCCESS = 0

C Primary loop in simulation
      DO 10 LINE = 1, TRIES, 1

C Tests whether neutron collides elastically with a
C hydrogen atom (see pg 79)

! may change this to AM/PU BESPEC()
         ENEU = AMBESPEC() ! sets initial neutron energy
         NPR = PROBS(ENEU)      ! sets probability of Hyd hit
         NPTOT = PROBS(ENEU) + PROBC(ENEU) ! total prob of interaction
         CHANCE = RAN1(IDUM)

         IF (CHANCE .LT. NPR) THEN

            SUCCESS = SUCCESS + 1
```

```
C Stores energy of the interacting neutron
            NEUOUT(ENEU)=NEUOUT(ENEU)+1

C Choose a random scattering angle...
            TANG = ANGLE(ENEU)

C Choose a random interaction distance (see pg 103 in logbook)
            DX = DIST1*RAN1(IDUM)
            DIST = DX / (COS((90-TANG)*.01745329252))

C Find proton energy
C For regular billiard-ball scatter
            T0 = REAL(ENEU)*(SIN(TANG*.01745329252)**2)/10.0
C /10 switches units to MeV

C Finds energy remaining in particle
            EREM = SCINTEN(DIST, T0)

C Updates energy lost in detector
            TEMP = 10.0*(T0-EREM)
            ELOSS(INT(TEMP))=ELOSS(INT(TEMP))+1

C Update number of partciles that went to next detector
C (Use an angular test here to see if angle < 20 degrees)
            IF (EREM .GT. 0.0 .AND. TANG .LT. 20.0) THEN
               PNEXT = PNEXT + 1
               TEMP = INT(10.0*EREM)
               ESORT(TEMP)=ESORT(TEMP)+1

C This looks at the same particles while they're still in the first det.
               TEMP = INT(10.0*(T0-EREM))
               EIN(TEMP)=EIN(TEMP)+1
            END IF

**************
C Second hydrogen scatter, only occurs once (see pg 103, 104)
            ENEU = ENEU * (COS(TANG*.01745329252))**2
            IF (ENEU .GT. 0) THEN
c            IF (.FALSE.) THEN ! to turn off secondary Hyd scatter
               IF (DX*TAN(TANG) .LT. 4.0) THEN
                  NEXTDIST = DX / COS(TANG*.01745329252)
               ELSE
                  NEXTDIST = 4.0 / COS(TANG*.01745329252)
               END IF
C This gives probability of proton scatter for ANY distance in plastic
               NPR = PROBSCAT(NEXTDIST, ENEU)
               CHANCE = RAN1(IDUM)

C second collision occurs!
               IF (CHANCE .LT. NPR) THEN
C geometry on pg 103 in logbook
                  TANG2 = ANGLE(ENEU)
                  DX2 = NEXTDIST*RAN1(IDUM)
! using small second angle approximation
                  DIST2P = DX2 / (COS((90-TANG2)*.01745329252))

C energy
                  T0 = REAL(ENEU)*(SIN(TANG2*.01745329252)**2)/10.0
                  EREM = SCINTEN(DIST2P, T0)
                  TEMP = 10.0*(T0-EREM)
                  ELOSS(INT(TEMP))=ELOSS(INT(TEMP))+1
               END IF
            END IF

**************
C Carbon Interaction!
         ELSE IF (CHANCE .LT. NPTOT) THEN
c         ELSE IF (.FALSE.) THEN ! to turn off the carbon scatter

            TANG = CANGLE(ENEU) ! TANG is in radians now in cm frame!
            ! and also this is for the neutron, not the carbon!
            ! ~= psi for m1 << m2
```

```
C Energy remaining pg 104 in logbook
            ENEU = ENEU*(MN*MN/((MN+MC)*(MN+MC))*(
     +           COS(TANG) + SQRT((MC/MN)*(MC/MN)-(SIN(TANG))**2))**2)

            DX = DIST1*RAN1(IDUM)

C some geometry (pg 104)
            IF (TANG .LT. 1.57079632679) THEN
               IF (DX*TAN(TANG) .LT. 4.0) THEN
                  NEXTDIST = DX / COS(TANG)
               ELSE
                  NEXTDIST = 4.0 / COS(TANG)
               END IF
            ELSE
               IF ((DIST1-DX)*TAN(TANG) .LT. 4.0) THEN
                  NEXTDIST = (DIST1-DX) / COS(TANG)
               ELSE
                  NEXTDIST = 4.0 / COS(TANG)
               END IF
            END IF

C Now proceeding as in 2nd hyd scatter
            NPR = PROBSCAT(NEXTDIST, ENEU)
            CHANCE = RAN1(IDUM)
C second collision occurs!
               IF (CHANCE .LT. NPR) THEN
C geometry
                  TANG2 = ANGLE(ENEU)

                  DX2 = NEXTDIST*RAN1(IDUM)
! using small angle approximation
                  DIST2P = DX2 / (COS((90-TANG2)*.01745329252))

C energy
                  T0 = REAL(ENEU)*(SIN(TANG2*.01745329252)**2)/10.0
                  EREM = SCINTEN(DIST2P, T0)
                  TEMP = 10.0*(T0-EREM)
                  ELOSS(INT(TEMP))=ELOSS(INT(TEMP))+1
               END IF

         END IF

**************


C Prints progress
         IF (MOD(LINE, 1000000) .EQ. 0) THEN
            PRINT *, 'Trial', LINE, ' done!'
         END IF

 10      CONTINUE

**************
C
C End of main loop!
C
**************


C Prints output
         PRINT *
         PRINT *, 'Number of Hydrogen collisions:'
         PRINT *, SUCCESS
         PRINT *
         PRINT *, 'Number of protons escaped with angle < 20 degrees:'
         PRINT *, PNEXT

C TOTAL file, which stores probability of proton recoil
      DO LINE = 1, 110, 1
         WRITE (2, *) PROBS(LINE)
      END DO
```

```
C Write EOUT file
      DO 40 LINE = 1, 110, 1
         WRITE (3, *) LINE, ESORT(LINE)
 40   CONTINUE

c Write ELOSS file... yawnnnn
      DO 50 LINE = 1, 110, 1
         WRITE (4, *) LINE, ELOSS(LINE)
 50   CONTINUE

C EIN file...
      DO 70 LINE = 1, 110, 1
         WRITE (8, *) LINE, EIN(LINE)
 70   CONTINUE

C NEUOUT file...
      DO 80 LINE = 1, 110, 1
         WRITE (10, *) LINE, NEUOUT(LINE)
 80   CONTINUE


**************
C Quenching logic (pg 105 in logbook)
C QUEN file:  Spreads out spectrum to match expected luminosity
      OPEN (UNIT = 31, FILE = 'QUEN')
      OPEN (UNIT = 32, FILE = 'LValues', STATUS = 'OLD')
      DO LINE = 1, 110, 1
         READ (32, *) TEMP
         QUEN(TEMP) = QUEN(TEMP) + ELOSS(LINE)
      END DO
      DO LINE = 1, 1100, 1
         IF (QUEN(LINE) .GT. 0) THEN
            WRITE (31, *) LINE, QUEN(LINE)
         END IF
      END DO
      END FILE (UNIT = 31)
      CLOSE (UNIT = 31)
      CLOSE (UNIT = 32)
**************


C Closes files
         END FILE (UNIT = 2)
         CLOSE (UNIT = 2)
         END FILE (UNIT = 3)
         CLOSE (UNIT = 3)
         END FILE (UNIT = 4)
         CLOSE (UNIT = 4)
         END FILE (UNIT = 8)
         CLOSE (UNIT = 8)
         END FILE (UNIT = 10)
         CLOSE (UNIT = 10)

C Ends program
      STOP
      END


*********************************************

      FUNCTION RAN1(IDUM)
C From Numerical Recipes 1989
C Has almost infinite period, but may be slow (ran2 faster)

C Returns a uniform random deviate between 0.0 and 1.0.
C Set IDUM to any negative value to initialize or
C reinitialize the sequence.

C Retyped by Jonathan Horton on Feb 17, 2005
C Seems to only work correctly when called from main program,
C not from subroutines.
```

```
      DIMENSION R(97)
      PARAMETER (M1=259200, IA1=7141, IC1=54773, RM1=1./M1)
      PARAMETER (M2=134456, IA2=8121, IC2=28411, RM2=1./M2)
      PARAMETER (M3=243000, IA3=4561, IC3=51349)
      DATA IFF /0/ ! Initialize on first call
      SAVE ! I added this line!


      IF (IDUM .LT. 0 .OR. IFF .EQ. 0) THEN
         IFF = 1
         IX1 = MOD(IC1 - IDUM, M1) ! seed first routine
         IX1 = MOD(IA1 * IX1 + IC1, M1)
         IX2 = MOD(IX1, M2) ! use it to seed second
         IX1 = MOD(IA1 * IX1 + IC1, M1)
         IX3 = MOD(IX1, M3) ! and third routines

         DO 11 J=1, 97 ! fill table with deviates from first
            IX1 = MOD(IA1 * IX1 + IC1, M1) ! two routines
            IX2 = MOD(IA2 * IX2 + IC2, M2)
            R(J) = (FLOAT(IX1) + FLOAT(IX2) * RM2)*RM1
C     Low and high order pieces combined here
 11      CONTINUE

         IDUM = 1
      END IF

      IX1 = MOD(IA1 * IX1 + IC1, M1) !Where starts after init
      IX2 = MOD(IA2 * IX2 + IC2, M2)
      IX3 = MOD(IA3 * IX3 + IC3, M3)

      J = 1 + (97 * IX3) / M3 !use 3rd seq to get int (1, 97)

      IF (J .GT. 97 .OR. J .LT. 1) PAUSE

      RAN1=R(J) ! return table entry
      R(J) = (FLOAT(IX1) + FLOAT(IX2) * RM2) * RM1 !refill

      RETURN
      END



****************************************

      REAL FUNCTION ANGLE(ENEU)
C Determines a random outgoing angle for a proton
C in an (n, p) collision.  This uses experimental
C data to determine probability of angle.

C Last update: 3/25/05

C Declarations
      INTEGER RUNS, TOSS, STOP, RAN, ENEU
      REAL X, Y, MU, FX, PI
      REAL A1(110), A2(110), A3(110), A4(110), A5(110), A6(110)
      REAL P1, P2, P3, P4, P5, P6
      PARAMETER (PI = 3.1415926535898)
      DATA RAN /1/
      SAVE

C Read in a file that stores the Legendre coeffs
      IF (RAN .EQ. 1) THEN
         OPEN (UNIT = 31, FILE = 'LegHyd', STATUS = 'OLD')

         DO LINE = 1, 110, 1
            READ (31, *) A1(LINE), A2(LINE), A3(LINE), A4(LINE),
     +           A5(LINE), A6(LINE)
         END DO

         RAN = 0
         CLOSE (UNIT = 31)
```

```
      END IF


      Y = 1.0 ! tricks loop to run
      FX = 0.0

C throwing darts method
      DO WHILE (Y .GT. FX)
C starts by generating a random angle
         X = PI*RAND(0)
         MU = COS(X)

C Inputting Legendre Polynomials for random angle chosen
         P1 = MU
         P2 = -.5 + 3.*MU*MU/2.
         P3 = -3.*MU/2. + 5.*MU*MU*MU/2.
         P4 = 3./8. - 15.*MU*MU/4. + 35.*MU*MU*MU*MU/8.
         P5 = 15.*MU/8. - 35.*MU*MU*MU/4. + 63.*MU**5/8.
         P6 = -5./16. + 105.*MU*MU/16. - 315.*MU**4/16.
     +        + 231.*MU**6/16.

C generates FX based on polynomials
         FX = .5 + 3./2.*A1(ENEU)*P1 + 5./2.*A2(ENEU)*P2
     +        + 7./2.*A3(ENEU)*P3 + 9./2.*A4(ENEU)*P4
     +        + 11./2.*A5(ENEU)*P5 + 13./2.*A6(ENEU)*P6

C finally creates a random y to test
         Y = RAND(0)

C restarts unless Y fall under FX curve generated
      END DO


C returns value in degrees, and converts from cm to lab for Hyd
      ANGLE = 90/PI*X


C End function
      RETURN
      END


****************************************

      REAL FUNCTION CANGLE(ENEU)
C Determines a random outgoing angle when a carbon atom is
C in a colision with a neutron.  This uses experimental
C data to determine probability of angle.

C Last update: 3/25/05

C Declarations
      INTEGER RUNS, TOSS, STOP, RAN, ENEU
      REAL X, Y, MU, FX, PI
      REAL A1(110), A2(110), A3(110), A4(110), A5(110), A6(110)
      REAL P1, P2, P3, P4, P5, P6
      PARAMETER (PI = 3.1415926535898)
      DATA RAN /1/
      SAVE

C Read in a file that stores the Legendre coeffs
      IF (RAN .EQ. 1) THEN
         OPEN (UNIT = 32, FILE = 'LegCar', STATUS = 'OLD')

         DO LINE = 1, 110, 1
            READ (32, *) A1(LINE), A2(LINE), A3(LINE), A4(LINE),
     +           A5(LINE), A6(LINE)
         END DO

         RAN = 0
         CLOSE (UNIT = 32)
      END IF
```

```
      Y = 1.0 ! tricks loop to run
      FX = 0.0

C throwing darts method
      DO WHILE (Y .GT. FX)
C starts by generating a random angle
         X = PI*RAND(0)
         MU = COS(X)

C Inputting Legendre Polynomials for random angle chosen
         P1 = MU
         P2 = -.5 + 3.*MU*MU/2.
         P3 = -3.*MU/2. + 5.*MU*MU*MU/2.
         P4 = 3./8. - 15.*MU*MU/4. + 35.*MU*MU*MU*MU/8.
         P5 = 15.*MU/8. - 35.*MU*MU*MU/4. + 63.*MU**5/8.
         P6 = -5./16. + 105.*MU*MU/16. - 315.*MU**4/16.
     +        + 231.*MU**6/16.

C generates FX based on polynomials
         FX = .5 + 3./2.*A1(ENEU)*P1 + 5./2.*A2(ENEU)*P2
     +        + 7./2.*A3(ENEU)*P3 + 9./2.*A4(ENEU)*P4
     +        + 11./2.*A5(ENEU)*P5 + 13./2.*A6(ENEU)*P6

C finally creates a random y to test
         Y = RAND(0)

C restarts unless Y fall under FX curve generated
      END DO

C returns value in radians, cm frame!!
      CANGLE = X

C End function
      RETURN
      END


****************************************

      REAL FUNCTION SCINTEN(DIST, T0)

C This function takes an initial energy T0
C in MeV, and distance traversed in cm, then
C returns the final energy.

C This is for energy loss in a plastic scintillator
C using approximation for loss (pg 76 in logbook)

C in: T0 in MeV, DIST in cm for Scintillator
C out: final energy in MeV

C Author: Jonathan Horton
C Last update: Feb 24, 2005

C Needed variables
      REAL T0, ALPHA, BETA, DIST, DEN, T, X

C Setting values for Plastic Scint
      PARAMETER(ALPHA = 0.002342)
      PARAMETER(BETA = 1.71677293994)
      PARAMETER(DEN = 1.032) ! g/cm3


C Converting the DIST units to usable units
      X = DIST * DEN

C Doing the calculation
C Make sure T .GT. 0
      IF (X .LT. ALPHA*(T0**BETA)) THEN
         SCINTEN = (T0 ** BETA - X / ALPHA)**(1 / BETA)
```

```
      ELSE
         SCINTEN = 0.0
      END IF

C Ends the function
      RETURN
      END

*****************************************

      INTEGER FUNCTION NEUSPEC()
C Generates a random neutron energy based on LENS simulations
C from Prof. Nann.  This is based on a 0 deg beam port with
C incident proton energy of 7.0 MeV on Be-9.  Uses the file
C entitled NEUSPEC

C Jonathan Horton
C 3/3/05


      INTEGER X, RAN
      REAL Y, ENEU(55)
      DATA RAN /1/
      SAVE

      NEUSPEC = 0.0

C This part runs only the first time
      IF (RAN .NE. 0) THEN
C     Opens neutron spectrum for neuspec function
         OPEN(UNIT = 9, FILE = 'NEUSPEC', STATUS = 'OLD')

C     Reads in probabilities for various neutron spectra for neuspec
         DO 3 LINE = 1, 55, 1
            READ (9, *) ENEU(LINE)
 3       CONTINUE

C     Closes the file...
         CLOSE(UNIT = 9)

         RAN = 0
      END IF

C Again, employing the throwing darts method...
      DO WHILE (NEUSPEC .EQ. 0.0)
         X = (RAND(0)*55 + 1)
         Y = RAND(0)*700.0

C Tests with stored probability file...
         IF (Y .LT. ENEU(X)) THEN
            NEUSPEC = X
         END IF

      END DO

      RETURN
      END


****************************************

      REAL FUNCTION HCROSS(ENEU)
C Loads cross sections for (n,p) elastic scattering
C in hydrogen, using the file HydCross.  If one sends
C it a Neutron energy in 100s of keV, then it will return
C the cross section for it.

C Jonathan Horton
C 3/4/05

      INTEGER RAN, ENEU
      DATA RAN /1/
```

```
      REAL HSIG(110)
      SAVE

C     Runs on first call only
      IF (RAN .EQ. 1) THEN
         OPEN(UNIT = 20, FILE = 'HydCross', STATUS = 'OLD')

C     Loads the stored data into an array for quick access
         DO 17 LINE = 1, 110, 1
            READ (20, *) HSIG(LINE)
 17       CONTINUE

         CLOSE(UNIT = 20)
         RAN = 0
      END IF

C Reports the requested cross section
      HCROSS = HSIG(ENEU)

      RETURN
      END


****************************************

      REAL FUNCTION CCROSS(ENEU)
C Loads cross sections for (n,p) elastic scattering
C in carbon, using the file CarCross.  If one sends
C it a Neutron energy in 100s of keV, then it will return
C the cross section for it.

C Jonathan Horton
C 3/4/05

      INTEGER RAN, ENEU
      DATA RAN /1/
      REAL CSIG(110)
      SAVE

C     Runs on first call only
      IF (RAN .EQ. 1) THEN
         OPEN(UNIT = 30, FILE = 'CarCross', STATUS = 'OLD')

C     Loads the stored data into an array for quick access
         DO 13 LINE = 1, 110, 1
            READ (30, *) CSIG(LINE)
 13      CONTINUE

         CLOSE(UNIT = 30)
         RAN = 0
      END IF

C Reports the requested cross section
      CCROSS = CSIG(ENEU)

      RETURN
      END


************************************

      SUBROUTINE NPROB(DIST1, PROBS, PROBC)

C Returns the probability array of
C an elastic collision with a hydrogen atom in a plastic scint
C Uses functions CarCross and HydCross.  Also needs distance in plastic.
C The first distance sent to it will generate the array.

C It not also returns the prob of elastic collision with Carbon
C in a plastic scint.  Calling this one time to generate arrays
C should speed up the program.
```

```
C Jonathan Horton
C 3/24/05

      REAL PROBS(110), NH, NC, DIST1, HC, CC, PROBC(110)
C Stores numbers of atoms for plastic scintillator
      PARAMETER(NH = 0.0524, NC = 0.0473)

      DO 37 LINE = 1, 110, 1

C Temporarily sets cross sections
         HC = HCROSS(LINE)
         CC = CCROSS(LINE)

C     Call cofunctions to generate array using equation on pg 79
         PROBS(LINE)=(NH*HC/(NH*HC+NC
     +         *CC))*(1-EXP(-(NH*HC+NC
     +         *CC)*DIST1))

C     One more time, now for carbon
         PROBC(LINE)=(NC*CC/(NH*HC+NC
     +         *CC))*(1-EXP(-(NH*HC+NC
     +         *CC)*DIST1))

 37   CONTINUE


      RETURN
      END

*********************************************
      FUNCTION PROBSCAT(NEXTDIST, ENEU)

C Returns the probability array of
C an elastic collision with a hydrogen atom in a plastic scint
C Uses functions CarCross and HydCross.  Also needs distance in plastic.

C It not also returns the prob of elastic collision with Carbon
C in a plastic scint.  Unlike the NPROB, this is called with ANY
C distance to give the probability. (for secondary collisions)

C Jonathan Horton
C 4/1/05

      REAL NH, NC, NEXTDIST, HC, CC
      INTEGER ENEU
C Stores numbers of atoms for plastic scintillator
      PARAMETER(NH = 0.0524, NC = 0.0473)

C Temporarily sets cross sections
      HC = HCROSS(ENEU)
      CC = CCROSS(ENEU)

C     Call cofunctions to generate array using equation on pg 79
      PROBSCAT=(NH*HC/(NH*HC+NC
     +     *CC))*(1-EXP(-(NH*HC+NC
     +     *CC)*NEXTDIST))

      RETURN
      END

*********************************************

      FUNCTION AMBESPEC()
C Generates a random neutron energy based on simulations
C from Kluge & Weise.  This is based on a standard AmBe
C source.  Uses the file entitled AmBeSpec

C Jonathan Horton
C 3/11/05


      INTEGER X, RAN
```

```
      REAL Y, ENEU(110)
      DATA RAN /1/
      SAVE

      AMBESPEC = 0

C This part runs only the first time
      IF (RAN .NE. 0) THEN
C     Opens neutron spectrum for neuspec function
         OPEN(UNIT = 11, FILE = 'AmBeSpec', STATUS = 'OLD')

C     Reads in probabilities for various neutron spectra for neuspec
         DO 3 LINE = 1, 110, 1
            READ (11, *) ENEU(LINE)
 3       CONTINUE

C     Closes the file...
         CLOSE(UNIT = 11)

         RAN = 0
      END IF

C Again, employing the throwing darts method...
      DO WHILE (AMBESPEC .EQ. 0.0)
         X = ((RAND(0)*110) + 1)
         Y = RAND(0)*0.2

C Tests with stored probability file...
         IF (Y .LT. ENEU(X)) THEN
            AMBESPEC = X
         END IF

      END DO

      RETURN
      END

**********************************

      FUNCTION PUBESPEC()
C Generates a random neutron energy based on simulations
C from L. Stewart.  This is based on a standard PuBe
C source.  Uses the file entitled PuBeSpec

C Jonathan Horton
C 3/11/05


      INTEGER X, RAN
      REAL Y, ENEU(110)
      DATA RAN /1/
      SAVE

      PUBESPEC = 0

C This part runs only the first time
      IF (RAN .NE. 0) THEN
C     Opens neutron spectrum for neuspec function
         OPEN(UNIT = 41, FILE = 'PuBeSpec', STATUS = 'OLD')

C     Reads in probabilities for various neutron spectra for neuspec
         DO 3 LINE = 1, 110, 1
            READ (41, *) ENEU(LINE)
 3       CONTINUE

C     Closes the file...
         CLOSE(UNIT = 41)

         RAN = 0
      END IF

C Again, employing the throwing darts method...
```

```
      DO WHILE (PUBESPEC .EQ. 0.0)
         X = ((RAND(0)*110) + 1)
         Y = RAND(0)*12.

C Tests with stored probability file...
         IF (Y .LT. ENEU(X)) THEN
            PUBESPEC = X
         END IF

      END DO

      RETURN
      END

**********************************
```

	Simulation Support Files					
CarCross	HydCross	LValues	AmBeSpec	PuBeSpec		
4.408399	12.765	2	0.1515	2.279		
4.115899	9.6609	3	0.1527	4.52		
3.855099	7.9678	5	0.1532	5.742		
3.618199	6.8912	7	0.15	6.611		
3.403299	6.1396	10	0.1428	7.262		
3.207599	5.5805	12	0.1345	7.534		
3.028999	5.1453	16	0.123	7.575		
2.865399	4.7945	19	0.1145	7.575		
2.715399	4.5042	23	0.1068	7.548		
2.577399	4.2586	27	0.1027	7.48		
2.450298	4.0471	32	0.0983	7.303		
2.333098	3.8625	36	0.0932	7.113		
2.224898	3.6992	41	0.0869	6.923		
2.124997	3.5533	46	0.0833	6.76		
2.032797	3.4219	52	0.0827	6.597		
1.946496	3.3025	58	0.086	6.475		
1.865496	3.1934	63	0.0923	6.38		
1.797995	3.0931	70	0.0977	6.312		
1.731895	3.0003	76	0.1015	6.299		
1.670395	2.9142	82	0.102	6.299		
2.215019	2.8339	89	0.1018	6.339		
1.631993	2.7588	96	0.102	6.434		
1.595292	2.6883	103	0.102	6.801		
1.582891	2.6219	110	0.1021	7.317		
1.59449	2.5592	118	0.1051	7.9		
1.639489	2.4999	125	0.1131	8.389		
1.739588	2.4436	133	0.1273	8.891		
2.037113	2.3902	141	0.1413	9.258		
2.615687	2.3393	149	0.1592	9.719		
1.170386	2.2907	157	0.1755	10.09		
1.582585	2.2453	165	0.1792	10.44		
1.990385	2.1999	174	0.1745	10.64		
2.313184	2.1583	182	0.1646	10.79		
2.541983	2.1166	191	0.1557	10.91		
2.640983	2.0782	200	0.1503	11		
2.608082	2.0398	209	0.1462	11.06		
2.479481	2.0042	218	0.1428	11.12		
2.30188	1.9686	227	0.1377	11.16		
2.11118	1.9355	236	0.1312	11.17		
1.932079	1.9024	246	0.1276	11.19		
1.812578	1.8715	255	0.1276	11.17		
2.004277	1.8406	265	0.1321	11.13		
2.219477	1.8117	275	0.1378	11.08		
1.893276	1.7828	285	0.1426	11		
1.667675	1.7557	295	0.1447	10.86		
1.517475	1.7286	305	0.1449	10.72		
1.403574	1.7031	315	0.1462	10.41		
1.307773	1.6775	325	0.1489	10.1		
1.222979	1.6535	336	0.1518	9.706		

1.120351	1.6294	346	0.1521	9.109
1.09193	1.6076	357	0.1467	8.593
1.020759	1.5857	367	0.1367	7.846
0.957168	1.5639	378	0.1264	7.1
1.202767	1.542	389	0.1182	6.719
0.990565	1.5202	400	0.1127	6.516
0.9588636	1.501	411	0.1084	6.367
0.9200614	1.4819	422	0.1026	6.204
0.9098593	1.4627	433	0.0949	6.136
0.8853571	1.4436	444	0.0855	6.122
0.875355	1.4244	456	0.08	6.136
0.8847192	1.4074	467	0.0792	6.163
0.9807917	1.3905	479	0.083	6.271
1.713168	1.3735	490	0.0886	6.421
0.8725991	1.3566	502	0.0926	6.543
0.8173893	1.3396	513	0.0923	6.652
0.514009	1.3245	525	0.0872	6.733
0.6555384	1.3093	537	0.0819	6.774
0.6464711	1.2942	549	0.0777	6.814
0.6132671	1.279	561	0.0755	6.828
0.5736164	1.2639	573	0.0748	6.842
0.5691353	1.2503	585	0.0761	6.828
0.6398751	1.2367	597	0.078	6.801
1.033445	1.2231	610	0.0801	6.76
1.413788	1.2095	622	0.0833	6.706
1.374824	1.1959	634	0.0855	6.611
1.335294	1.1836	647	0.087	6.529
1.529955	1.1713	659	0.0875	6.421
1.629494	1.1591	672	0.0846	6.231
1.467995	1.1468	684	0.0806	6.041
1.350856	1.1345	697	0.0738	5.783
1.317188	1.1233	710	0.0664	5.457
0.9730368	1.1121	722	0.0574	5.023
0.8557012	1.101	735	0.0486	4.398
0.7975151	1.0898	748	0.0407	3.557
0.7491042	1.0786	761	0.0313	3.109
0.7552142	1.0684	774	0.0265	2.796
0.7451351	1.0582	787	0.0215	2.593
0.706846	1.0481	800	0.0185	2.416
0.6554212	1.0379	813	0.0167	2.321
0.6306779	1.0277	826	0.0155	2.267
0.6965786	1.0184	840	0.0152	2.226
0.7333392	1.009	853	0.0161	2.213
0.7169557	0.99972	866	0.019	2.199
0.6813887	0.99039	880	0.0223	2.226
0.6693117	0.98106	893	0.0252	2.267
0.6714841	0.97248	907	0.0274	2.335
0.6854558	0.9639	920	0.0277	2.376
0.6845276	0.95532	934	0.0267	2.321
0.6717994	0.94674	947	0.0242	2.213
0.6567711	0.93816	961	0.022	1.955
0.6389638	0.93024	975	0.0197	1.71

0.639185		0.92232		989		0.0179	1.412
0.628637		0.91441		1002		0.0169	1.14
0.6433191		0.90649		1016		0.0149	0.8959
0.6909111		0.89857		1030		0.0123	0.5973
0.7204084		0.89124		1044		0.0095	0.3258
0.7526048		0.88392		1058		0.0065	0.01357
0.8128466		0.87659		1072		0.0038	0
0.8733984		0.86927		1086		0.0015	0
0.8621401		0.86194		1100		0.0008	0

LegHyd					
-1.786000E-04	2.875800E-07	-1.830800E-10	1.387800E-13	1.136700E-14	-6.187900E-15
-3.362900E-04	1.398300E-06	-1.293300E-09	3.131800E-12	2.076900E-14	-1.235300E-14
-4.797000E-04	3.592200E-06	-3.913500E-09	1.915100E-11	3.934900E-14	-1.767200E-14
-6.132400E-04	7.028700E-06	-8.434300E-09	6.938500E-11	7.696900E-14	-2.279900E-14
-7.399400E-04	1.180500E-05	-1.517200E-08	1.883500E-10	1.746000E-13	-2.810800E-14
-8.619700E-04	1.797800E-05	-2.443500E-08	4.255700E-10	3.956800E-13	-3.076900E-14
-9.808800E-04	2.557900E-05	-3.656800E-08	8.468400E-10	8.467300E-13	-2.928400E-14
-1.097800E-03	3.461700E-05	-5.197100E-08	1.535300E-09	1.684000E-12	-1.790700E-14
-1.213600E-03	4.509400E-05	-7.112300E-08	2.592200E-09	3.124300E-12	1.191300E-14
-1.328900E-03	5.699700E-05	-9.458400E-08	4.138000E-09	5.456000E-12	7.247800E-14
-1.444200E-03	7.031000E-05	-1.230100E-07	6.312500E-09	9.047300E-12	1.809500E-13
-1.559900E-03	8.501200E-05	-1.571400E-07	9.275900E-09	1.436300E-11	3.608700E-13
-1.676200E-03	1.010700E-04	-1.978300E-07	1.320900E-08	2.197000E-11	6.500900E-13
-1.793400E-03	1.184700E-04	-2.460200E-07	1.831400E-08	3.255000E-11	1.093300E-12
-1.911600E-03	1.371700E-04	-3.027600E-07	2.481500E-08	4.690400E-11	1.751500E-12
-2.030900E-03	1.571400E-04	-3.691900E-07	3.295700E-08	6.596600E-11	2.702200E-12
-2.151500E-03	1.783500E-04	-4.465600E-07	4.300700E-08	9.081200E-11	4.042200E-12
-2.273300E-03	2.007700E-04	-5.362000E-07	5.525600E-08	1.226600E-10	5.893400E-12
-2.396400E-03	2.243500E-04	-6.395600E-07	7.001700E-08	1.628800E-10	8.400600E-12
-2.520800E-03	2.490800E-04	-7.581600E-07	8.762500E-08	2.130200E-10	1.174500E-11
-2.646500E-03	2.749000E-04	-8.936500E-07	1.084400E-07	2.747700E-10	1.614100E-11
-2.773600E-03	3.017900E-04	-1.047700E-06	1.328400E-07	3.500000E-10	2.184500E-11
-2.902000E-03	3.297100E-04	-1.222300E-06	1.612300E-07	4.407500E-10	2.915300E-11
-3.031600E-03	3.586300E-04	-1.419100E-06	1.940300E-07	5.492400E-10	3.842100E-11
-3.162500E-03	3.885100E-04	-1.640200E-06	2.317100E-07	6.778400E-10	5.005400E-11
-3.294600E-03	4.193200E-04	-1.887700E-06	2.747200E-07	8.291300E-10	6.452500E-11
-3.427900E-03	4.510300E-04	-2.163800E-06	3.235600E-07	1.005800E-09	8.237600E-11
-3.562300E-03	4.835900E-04	-2.470700E-06	3.787600E-07	1.210800E-09	1.042200E-10
-3.697800E-03	5.169900E-04	-2.810600E-06	4.408400E-07	1.447200E-09	1.307600E-10
-3.834300E-03	5.511800E-04	-3.186100E-06	5.103800E-07	1.718200E-09	1.627900E-10
-3.834300E-03	5.511800E-04	-3.186100E-06	5.103800E-07	1.718200E-09	1.627900E-10
-4.110200E-03	6.218100E-04	-4.053500E-06	6.741500E-07	2.377500E-09	2.469900E-10
-4.110200E-03	6.218100E-04	-4.053500E-06	6.741500E-07	2.377500E-09	2.469900E-10
-4.389700E-03	6.952500E-04	-5.093600E-06	8.749900E-07	3.217400E-09	3.653100E-10
-4.389700E-03	6.952500E-04	-5.093600E-06	8.749900E-07	3.217400E-09	3.653100E-10
-4.672300E-03	7.712300E-04	-6.327900E-06	1.118100E-06	4.268100E-09	5.282500E-10
-4.672300E-03	7.712300E-04	-6.327900E-06	1.118100E-06	4.268100E-09	5.282500E-10
-4.957600E-03	8.495200E-04	-7.779400E-06	1.409100E-06	5.561500E-09	7.486500E-10
-4.957600E-03	8.495200E-04	-7.779400E-06	1.409100E-06	5.561500E-09	7.486500E-10
-5.245200E-03	9.299000E-04	-9.471700E-06	1.753900E-06	7.129800E-09	1.042000E-09
-5.245200E-03	9.299000E-04	-9.471700E-06	1.753900E-06	7.129800E-09	1.042000E-09
-5.534600E-03	1.012100E-03	-1.142900E-05	2.158400E-06	9.005600E-09	1.426900E-09
-5.534600E-03	1.012100E-03	-1.142900E-05	2.158400E-06	9.005600E-09	1.426900E-09
-5.825500E-03	1.096000E-03	-1.367700E-05	2.629300E-06	1.122000E-08	1.925200E-09
-5.825500E-03	1.096000E-03	-1.367700E-05	2.629300E-06	1.122000E-08	1.925200E-09
-6.117400E-03	1.181300E-03	-1.624200E-05	3.173000E-06	1.380400E-08	2.562700E-09
-6.117400E-03	1.181300E-03	-1.624200E-05	3.173000E-06	1.380400E-08	2.562700E-09
-6.409900E-03	1.267800E-03	-1.915000E-05	3.796500E-06	1.678300E-08	3.369400E-09
-6.409900E-03	1.267800E-03	-1.915000E-05	3.796500E-06	1.678300E-08	3.369400E-09

-6.702800E-03	1.355300E-03	-2.242900E-05	4.506800E-06	2.017900E-08	4.380000E-09
-6.702800E-03	1.355300E-03	-2.242900E-05	4.506800E-06	2.017900E-08	4.380000E-09
-6.702800E-03	1.355300E-03	-2.242900E-05	4.506800E-06	2.017900E-08	4.380000E-09
-6.702800E-03	1.355300E-03	-2.242900E-05	4.506800E-06	2.017900E-08	4.380000E-09
-7.433800E-03	1.577500E-03	-3.242800E-05	6.710700E-06	3.059300E-08	8.074200E-09
-7.433800E-03	1.577500E-03	-3.242800E-05	6.710700E-06	3.059300E-08	8.074200E-09
-7.433800E-03	1.577500E-03	-3.242800E-05	6.710700E-06	3.059300E-08	8.074200E-09
-7.433800E-03	1.577500E-03	-3.242800E-05	6.710700E-06	3.059300E-08	8.074200E-09
-7.433800E-03	1.577500E-03	-3.242800E-05	6.710700E-06	3.059300E-08	8.074200E-09
-8.158900E-03	1.802300E-03	-4.535600E-05	9.620600E-06	4.373800E-08	1.409400E-08
-8.158900E-03	1.802300E-03	-4.535600E-05	9.620600E-06	4.373800E-08	1.409400E-08
-8.158900E-03	1.802300E-03	-4.535600E-05	9.620600E-06	4.373800E-08	1.409400E-08
-8.158900E-03	1.802300E-03	-4.535600E-05	9.620600E-06	4.373800E-08	1.409400E-08
-8.158900E-03	1.802300E-03	-4.535600E-05	9.620600E-06	4.373800E-08	1.409400E-08
-8.873400E-03	2.027300E-03	-6.165800E-05	1.335800E-05	5.919400E-08	2.349800E-08
-8.873400E-03	2.027300E-03	-6.165800E-05	1.335800E-05	5.919400E-08	2.349800E-08
-8.873400E-03	2.027300E-03	-6.165800E-05	1.335800E-05	5.919400E-08	2.349800E-08
-8.873400E-03	2.027300E-03	-6.165800E-05	1.335800E-05	5.919400E-08	2.349800E-08
-8.873400E-03	2.027300E-03	-6.165800E-05	1.335800E-05	5.919400E-08	2.349800E-08
-9.573000E-03	2.250400E-03	-8.177900E-05	1.804400E-05	7.587300E-08	3.766600E-08
-9.573000E-03	2.250400E-03	-8.177900E-05	1.804400E-05	7.587300E-08	3.766600E-08
-9.573000E-03	2.250400E-03	-8.177900E-05	1.804400E-05	7.587300E-08	3.766600E-08
-9.573000E-03	2.250400E-03	-8.177900E-05	1.804400E-05	7.587300E-08	3.766600E-08
-9.573000E-03	2.250400E-03	-8.177900E-05	1.804400E-05	7.587300E-08	3.766600E-08
-1.025400E-02	2.469800E-03	-1.061500E-04	2.380200E-05	9.178600E-08	5.835400E-08
-1.025400E-02	2.469800E-03	-1.061500E-04	2.380200E-05	9.178600E-08	5.835400E-08
-1.025400E-02	2.469800E-03	-1.061500E-04	2.380200E-05	9.178600E-08	5.835400E-08
-1.025400E-02	2.469800E-03	-1.061500E-04	2.380200E-05	9.178600E-08	5.835400E-08
-1.025400E-02	2.469800E-03	-1.061500E-04	2.380200E-05	9.178600E-08	5.835400E-08
-1.091300E-02	2.683900E-03	-1.352000E-04	3.075000E-05	1.037700E-07	8.775100E-08
-1.091300E-02	2.683900E-03	-1.352000E-04	3.075000E-05	1.037700E-07	8.775100E-08
-1.091300E-02	2.683900E-03	-1.352000E-04	3.075000E-05	1.037700E-07	8.775100E-08
-1.091300E-02	2.683900E-03	-1.352000E-04	3.075000E-05	1.037700E-07	8.775100E-08
-1.091300E-02	2.683900E-03	-1.352000E-04	3.075000E-05	1.037700E-07	8.775100E-08
-1.154700E-02	2.891400E-03	-1.693000E-04	3.899900E-05	1.071600E-07	1.285300E-07
-1.154700E-02	2.891400E-03	-1.693000E-04	3.899900E-05	1.071600E-07	1.285300E-07
-1.154700E-02	2.891400E-03	-1.693000E-04	3.899900E-05	1.071600E-07	1.285300E-07
-1.154700E-02	2.891400E-03	-1.693000E-04	3.899900E-05	1.071600E-07	1.285300E-07
-1.154700E-02	2.891400E-03	-1.693000E-04	3.899900E-05	1.071600E-07	1.285300E-07
-1.215400E-02	3.091200E-03	-2.088200E-04	4.865400E-05	9.550800E-08	1.838900E-07
-1.215400E-02	3.091200E-03	-2.088200E-04	4.865400E-05	9.550800E-08	1.838900E-07
-1.215400E-02	3.091200E-03	-2.088200E-04	4.865400E-05	9.550800E-08	1.838900E-07
-1.215400E-02	3.091200E-03	-2.088200E-04	4.865400E-05	9.550800E-08	1.838900E-07
-1.215400E-02	3.091200E-03	-2.088200E-04	4.865400E-05	9.550800E-08	1.838900E-07
-1.273100E-02	3.282500E-03	-2.540700E-04	5.980900E-05	6.016700E-08	2.576000E-07
-1.273100E-02	3.282500E-03	-2.540700E-04	5.980900E-05	6.016700E-08	2.576000E-07
-1.273100E-02	3.282500E-03	-2.540700E-04	5.980900E-05	6.016700E-08	2.576000E-07
-1.273100E-02	3.282500E-03	-2.540700E-04	5.980900E-05	6.016700E-08	2.576000E-07
-1.273100E-02	3.282500E-03	-2.540700E-04	5.980900E-05	6.016700E-08	2.576000E-07
-1.327700E-02	3.464700E-03	-3.053300E-04	7.254700E-05	-1.005200E-08	3.540700E-07
-1.327700E-02	3.464700E-03	-3.053300E-04	7.254700E-05	-1.005200E-08	3.540700E-07
-1.327700E-02	3.464700E-03	-3.053300E-04	7.254700E-05	-1.005200E-08	3.540700E-07

-1.327700E-02	3.464700E-03	-3.053300E-04	7.254700E-05	-1.005200E-08	3.540700E-07
-1.327700E-02	3.464700E-03	-3.053300E-04	7.254700E-05	-1.005200E-08	3.540700E-07
-1.379100E-02	3.637400E-03	-3.628100E-04	8.693800E-05	-1.293000E-07	4.782900E-07
-1.379100E-02	3.637400E-03	-3.628100E-04	8.693800E-05	-1.293000E-07	4.782900E-07
-1.379100E-02	3.637400E-03	-3.628100E-04	8.693800E-05	-1.293000E-07	4.782900E-07
-1.379100E-02	3.637400E-03	-3.628100E-04	8.693800E-05	-1.293000E-07	4.782900E-07
-1.379100E-02	3.637400E-03	-3.628100E-04	8.693800E-05	-1.293000E-07	4.782900E-07
-1.427100E-02	3.800500E-03	-4.266800E-04	1.030300E-04	-3.150700E-07	6.359500E-07
-1.427100E-02	3.800500E-03	-4.266800E-04	1.030300E-04	-3.150700E-07	6.359500E-07

LegCar					
1.245700E-02	2.801300E-04	0.000000E+00	0.000000E+00	0.000000E+00	0.000000E+00
2.486800E-02	1.014300E-03	0.000000E+00	0.000000E+00	0.000000E+00	0.000000E+00
3.389700E-02	1.946500E-03	6.334400E-05	0.000000E+00	0.000000E+00	0.000000E+00
4.148600E-02	3.011600E-03	1.281000E-04	0.000000E+00	0.000000E+00	0.000000E+00
4.780200E-02	4.132600E-03	2.230800E-04	0.000000E+00	0.000000E+00	0.000000E+00
5.314500E-02	5.274000E-03	3.476700E-04	0.000000E+00	0.000000E+00	0.000000E+00
5.744800E-02	6.394900E-03	4.974000E-04	-5.641100E-05	0.000000E+00	0.000000E+00
6.078900E-02	7.486100E-03	6.650900E-04	-1.013500E-04	0.000000E+00	0.000000E+00
6.322600E-02	8.553600E-03	8.401900E-04	-1.700600E-04	0.000000E+00	0.000000E+00
6.479700E-02	9.618100E-03	1.008100E-03	-2.704900E-04	0.000000E+00	0.000000E+00
6.550000E-02	1.070900E-02	1.146800E-03	-4.118800E-04	0.000000E+00	0.000000E+00
6.536000E-02	1.188100E-02	1.234700E-03	-6.050800E-04	0.000000E+00	0.000000E+00
6.436300E-02	1.319900E-02	1.240500E-03	-8.620300E-04	0.000000E+00	0.000000E+00
6.247500E-02	1.475200E-02	1.122800E-03	-1.195200E-03	6.114500E-05	0.000000E+00
5.963500E-02	1.664300E-02	8.259800E-04	-1.615700E-03	8.828800E-05	0.000000E+00
5.578100E-02	1.897000E-02	2.492400E-04	-2.126300E-03	1.247900E-04	0.000000E+00
5.076500E-02	2.158000E-02	-8.678800E-04	-2.658500E-03	1.728200E-04	0.000000E+00
4.347500E-02	2.586000E-02	-2.104400E-03	-3.316800E-03	2.341100E-04	0.000000E+00
3.462400E-02	3.058600E-02	-5.085300E-03	-3.596600E-03	3.065600E-04	0.000000E+00
1.816100E-02	3.648000E-02	-1.332200E-02	-1.006900E-03	3.530600E-04	0.000000E+00
3.059567E-02	1.612497E-01	6.874667E-03	6.562778E-03	6.056570E-04	0.000000E+00
3.352500E-02	7.223900E-02	7.923800E-03	-1.615600E-02	8.432400E-04	0.000000E+00
6.206700E-03	8.469710E-02	-4.603100E-03	-1.697100E-02	1.109700E-03	0.000000E+00
-1.572700E-02	1.180300E-01	-1.182800E-02	-2.089400E-02	1.541800E-03	0.000000E+00
-1.572700E-02	1.180300E-01	-1.182800E-02	-2.089400E-02	1.541800E-03	0.000000E+00
-3.655900E-02	1.684700E-01	-1.863200E-02	-2.550600E-02	2.040700E-03	0.000000E+00
-4.791300E-02	2.415900E-01	-2.207500E-02	-2.924100E-02	2.102900E-03	0.000000E+00
-2.816600E-02	2.684900E-01	-1.352800E-02	-3.224100E-02	-2.143700E-04	2.081800E-04
-3.385000E-02	3.644500E-01	-1.328300E-02	-1.771900E-02	2.856400E-03	-8.198900E-05
7.872310E-02	4.029700E-02	5.622400E-02	1.844600E-02	0.000000E+00	0.000000E+00
-7.009800E-02	2.193400E-01	-2.348800E-02	-3.036900E-02	4.576600E-03	-1.340200E-04
-6.205300E-02	3.309700E-01	-2.133700E-02	-2.723200E-02	4.487100E-03	-1.138200E-04
-4.077700E-02	3.682500E-01	-1.014700E-02	-1.950200E-02	3.891800E-03	-1.115400E-04
-1.657200E-02	3.823000E-01	3.931300E-03	-1.027300E-02	3.028700E-03	-1.163400E-04
6.739100E-03	3.803400E-01	1.911300E-02	-5.874600E-04	1.975000E-03	-1.286100E-04
2.632600E-02	3.674100E-01	3.410800E-02	8.834100E-03	8.050000E-04	-1.495200E-04
4.016800E-02	3.475100E-01	4.801900E-02	1.759300E-02	-4.245900E-04	-1.803100E-04
4.670500E-02	3.233200E-01	6.021800E-02	2.558900E-02	-1.681400E-03	-2.222200E-04
4.448100E-02	2.957800E-01	7.000710E-02	3.297100E-02	-2.954900E-03	-2.765700E-04
3.360800E-02	2.627000E-01	7.576000E-02	4.010500E-02	-4.239000E-03	-3.441000E-04
3.506800E-02	2.137400E-01	7.227410E-02	4.701700E-02	-5.413900E-03	-4.165800E-04
2.136500E-01	1.419500E-01	5.589800E-02	4.674400E-02	-5.586600E-03	-4.268000E-04
4.446100E-01	1.606400E-01	8.098800E-02	3.630700E-02	-5.595400E-03	-4.356000E-04
3.980900E-01	1.866700E-01	1.086900E-01	3.770800E-02	-7.149500E-03	-5.757700E-04
3.446600E-01	1.860100E-01	1.223600E-01	4.110000E-02	-8.751400E-03	-7.354300E-04
3.115100E-01	1.774500E-01	1.309900E-01	4.378500E-02	-1.029800E-02	-9.074100E-04
2.899700E-01	1.666200E-01	1.372800E-01	4.575300E-02	-1.187100E-02	-1.099300E-03
2.743300E-01	1.545400E-01	1.412700E-01	4.720000E-02	-1.355100E-02	-1.319900E-03
2.590700E-01	1.339700E-01	1.322400E-01	4.885300E-02	-1.567700E-02	-1.605200E-03

2.460000E-01	1.244000E-01	1.080000E-01	4.000000E-02	-3.000000E-03	0.000000E+00
2.460000E-01	1.244000E-01	1.080000E-01	4.000000E-02	-3.000000E-03	0.000000E+00
2.350000E-01	1.063000E-01	9.200010E-02	3.716000E-02	-5.670000E-03	0.000000E+00
2.420000E-01	1.000000E-01	4.700000E-02	3.574000E-02	-7.330000E-03	0.000000E+00
3.195000E-01	1.883100E-01	1.220000E-01	3.339000E-02	-9.000000E-03	0.000000E+00
2.186200E-01	1.798700E-01	1.400000E-01	3.073000E-02	-1.200000E-02	0.000000E+00
2.080000E-01	1.756600E-01	1.402500E-01	2.940000E-02	-1.350000E-02	0.000000E+00
1.943300E-01	1.630000E-01	1.410000E-01	2.460000E-02	-1.800000E-02	0.000000E+00
1.715600E-01	1.615000E-01	1.440000E-01	1.660000E-02	-2.800000E-02	0.000000E+00
1.715600E-01	1.615000E-01	1.440000E-01	1.660000E-02	-2.800000E-02	0.000000E+00
1.630000E-01	1.630000E-01	1.600000E-01	1.400000E-02	-3.294000E-02	0.000000E+00
1.550000E-01	1.670000E-01	1.790000E-01	1.300000E-02	-3.588000E-02	2.000000E-03
1.188500E-01	1.828700E-01	2.243000E-01	2.080000E-02	-4.000000E-02	1.700000E-02
2.112000E-01	2.590000E-01	2.680000E-01	1.608000E-01	5.850000E-02	3.200000E-02
3.634800E-01	2.767500E-01	1.760000E-01	1.475900E-01	6.136000E-02	1.000000E-02
4.500000E-01	3.060000E-01	1.901900E-01	1.115000E-01	3.500000E-02	-4.670000E-03
3.000000E-01	1.700000E-01	1.950000E-01	1.167500E-01	1.700000E-02	5.000000E-03
2.138000E-01	9.500010E-02	1.430000E-01	8.300000E-02	3.000000E-03	2.000000E-03
1.998700E-01	6.483000E-02	1.190000E-01	5.700000E-02	-8.000000E-03	0.000000E+00
1.958600E-01	4.500000E-02	8.700010E-02	3.100000E-02	-1.400000E-02	0.000000E+00
2.067500E-01	4.300000E-02	7.300000E-02	2.500000E-02	-1.300000E-02	0.000000E+00
2.640000E-01	5.680000E-02	4.033000E-02	1.900000E-02	-5.200000E-03	0.000000E+00
4.098500E-01	1.400000E-01	4.700000E-02	2.100000E-02	2.750000E-03	0.000000E+00
6.360000E-01	3.133300E-01	1.015000E-01	2.600000E-02	1.225000E-02	0.000000E+00
4.836700E-01	4.300000E-01	1.590000E-01	3.400000E-02	2.100000E-02	0.000000E+00
3.170000E-01	4.380000E-01	1.915000E-01	4.800000E-02	2.200000E-02	5.700000E-04
2.790000E-01	4.058600E-01	2.135700E-01	9.035000E-02	2.300000E-02	7.500000E-03
2.701000E-01	4.300000E-01	2.307100E-01	1.248000E-01	5.939000E-02	1.350000E-02
3.418200E-01	5.430000E-01	2.478600E-01	1.330000E-01	8.400000E-02	3.770000E-03
4.463600E-01	5.543300E-01	2.564300E-01	1.333300E-01	6.667000E-02	-2.000000E-03
5.000000E-01	5.000000E-01	2.400000E-01	1.000000E-01	2.400000E-02	-1.200000E-02
6.337000E-01	5.299000E-01	3.526000E-01	2.108000E-01	8.000000E-02	8.000000E-03
6.548000E-01	5.360000E-01	3.612000E-01	2.180000E-01	8.000000E-02	8.000000E-03
6.510000E-01	5.000000E-01	3.523000E-01	2.067000E-01	6.625010E-02	7.330000E-03
5.674000E-01	4.400000E-01	3.321000E-01	1.689000E-01	4.000000E-02	5.110000E-03
4.600000E-01	3.600000E-01	3.000000E-01	1.100000E-01	4.000000E-03	1.000000E-03
4.600000E-01	3.600000E-01	3.000000E-01	1.100000E-01	4.000000E-03	1.000000E-03
3.745000E-01	3.338000E-01	3.019000E-01	1.015000E-01	1.371000E-02	1.648000E-02
3.745000E-01	3.338000E-01	3.019000E-01	1.015000E-01	1.371000E-02	1.648000E-02
2.800000E-01	2.300000E-01	2.900000E-01	9.000000E-02	1.000000E-03	5.000000E-03
2.800000E-01	2.300000E-01	2.900000E-01	9.000000E-02	1.000000E-03	5.000000E-03
2.800000E-01	2.300000E-01	2.900000E-01	9.000000E-02	1.000000E-03	5.000000E-03
2.800000E-01	2.300000E-01	2.900000E-01	9.000000E-02	1.000000E-03	5.000000E-03
2.800000E-01	2.300000E-01	2.900000E-01	9.000000E-02	1.000000E-03	5.000000E-03
4.600000E-01	3.800000E-01	3.100000E-01	1.400000E-01	4.000000E-02	5.000000E-03
4.600000E-01	3.800000E-01	3.100000E-01	1.400000E-01	4.000000E-02	5.000000E-03
4.600000E-01	3.800000E-01	3.100000E-01	1.400000E-01	4.000000E-02	5.000000E-03
4.600000E-01	3.800000E-01	3.100000E-01	1.400000E-01	4.000000E-02	5.000000E-03
4.600000E-01	3.800000E-01	3.100000E-01	1.400000E-01	4.000000E-02	5.000000E-03
5.500000E-01	4.200000E-01	3.300000E-01	1.500000E-01	3.000000E-02	6.000000E-03
5.500000E-01	4.200000E-01	3.300000E-01	1.500000E-01	3.000000E-02	6.000000E-03
5.500000E-01	4.200000E-01	3.300000E-01	1.500000E-01	3.000000E-02	6.000000E-03

5.500000E-01	4.200000E-01	3.300000E-01	1.500000E-01	3.000000E-02	6.000000E-03
5.500000E-01	4.200000E-01	3.300000E-01	1.500000E-01	3.000000E-02	6.000000E-03
5.300000E-01	4.300000E-01	3.300000E-01	1.300000E-01	4.000000E-02	3.500000E-02
5.300000E-01	4.300000E-01	3.300000E-01	1.300000E-01	4.000000E-02	3.500000E-02
5.300000E-01	4.300000E-01	3.300000E-01	1.300000E-01	4.000000E-02	3.500000E-02
5.300000E-01	4.300000E-01	3.300000E-01	1.300000E-01	4.000000E-02	3.500000E-02
5.300000E-01	4.300000E-01	3.300000E-01	1.300000E-01	4.000000E-02	3.500000E-02
6.000000E-01	4.600000E-01	3.200000E-01	1.300000E-01	4.000000E-02	1.000000E-02
6.000000E-01	4.600000E-01	3.200000E-01	1.300000E-01	4.000000E-02	1.000000E-02